# Single-step, acid-based fabrication of homogeneous gelatin-polycaprolactone fibrillar scaffolds intended for skin tissue engineering

# Single-step, acid-based fabrication of homogeneous gelatin-polycaprolactone fibrillar scaffolds intended for skin tissue engineering

Gina Prado-Prone[a,b] (PhD, gpradoprone@gmail.com), Masoomeh Bazzar[c,d] (PhD, m.bazzar@uea.ac.uk), Maria Letizia Focarete[d,e] (PhD, marialetizia.focarete@unibo.it), Jorge A. García-Macedo[f] (PhD, gamaj@fisica.unam.mx), Javier Perez-Orive[g] (PhD, jperezo@inr.gob.mx), Clemente Ibarra (PhD, cibarra@inr.gob.mx)[h], Cristina Velasquillo[i,*] (PhD, mvelasquillo@inr.gob.mx) and Phaedra Silva-Bermudez[b,*] (PhD, phaedrasilva@yahoo.com).

[a]*División de Estudios de Posgrado e Investigación, Facultad de Odontología, Universidad Nacional Autónoma de México; Ciudad Universitaria No. 3000, C.P. 04360, Ciudad de México, México.*
[b]*Unidad de Ingeniería de Tejidos, Terapia Celular y Medicina Regenerativa; Instituto Nacional de Rehabilitación Luis Guillermo Ibarra Ibarra; Av. México Xochimilco No. 289 Col. Arenal de Guadalupe C.P. 14389, Ciudad de México, México.*
[c]*School of Chemistry, University of East Anglia, Norwich, United Kingdom.*
[d]*Department of Chemistry "G. Ciamician" and National Consortium of Materials Science and Technology (INSTM, Bologna RU), Alma Mater Studiorum - Università di Bologna, 40126 Bologna, Italy*
[e]*Health Sciences and Technologies – Interdepartmental Center for Industrial Research (HST-ICIR), Alma Mater Studiorum - Università di Bologna, 40064 Ozzano dell'Emilia, Bologna, Italy*
[f]*Departamento de Estado Sólido, Instituto de Física, Universidad Nacional Autónoma de México; Ciudad Universitaria No. 3000, C.P. 04360, Ciudad de México, México.*
[g]*Dirección de Investigación, Instituto Nacional de Rehabilitación Luis Guillermo Ibarra Ibarra; Av. México Xochimilco No. 289 Col. Arenal de Guadalupe C.P. 14389, Ciudad de México, México.*
[h]*Dirección General, Instituto Nacional de Rehabilitación Luis Guillermo Ibarra Ibarra, Ciudad de México, México.*
[i]*Biotecnología, Instituto Nacional de Rehabilitación Luis Guillermo Ibarra Ibarra; Av. México Xochimilco No. 289 Col. Arenal de Guadalupe C.P. 14389, Ciudad de México, México.*

**Competing Interests**

The authors declare that no competing interests are present, and there is no conflict of interest.

*Corresponding authors: C. Velasquillo at m.velasquillo@inr.gob.mx and P. Silva-Bermudez at phaedrasilva@yahoo.com or pssilva@inr.gob.mx

## Abstract

Blends of natural and synthetic polymers have recently attracted great attention as scaffolds for tissue engineering applications due to their favorable biological and mechanical properties. Nevertheless, phase-separation of blend components is an important challenge facing the development of electrospun homogeneous fibrillar natural-synthetic polymers scaffolds; phase-separation can produce significant detrimental effects for scaffolds fabricated by electrospinning. In the present study, blends of gelatin (Gel; natural polymer) and polycaprolactone (PCL; synthetic polymer), containing 30 and 45 wt.% Gel, were prepared using acetic acid as a "green" sole solvent to straightforwardly produce appropriate single-step Gel-PCL solutions for electrospinning. Miscibility of Gel and PCL in the scaffolds was assessed and the morphology, chemical composition and structural and solid-state properties of the scaffolds were thoroughly investigated. Results showed that the two polymers proved miscible under the single-step solution process used and that the electrospun scaffolds presented suitable properties for potential skin tissue engineering applications. Viability, metabolic activity and protein expression of human fibroblasts cultured on the Gel-PCL scaffolds were evaluated using LIVE/DEAD (calcein/ethidium homodimer), MTT-Formazan and immunocytochemistry assays, respectively. *In vitro* results showed that the electrospun Gel-PCL scaffolds enhanced cell viability and proliferation in comparison to PCL scaffolds. Furthermore, scaffolds allowed fibroblasts expression of extracellular matrix proteins, tropoelastin and collagen Type I, in a similar way to positive controls. Results indicated the feasibility of the single-step solution process used herein to obtain homogeneous electrospun Gel-PCL scaffolds with Gel content ≥ 30 wt.% and potential properties to be used as scaffolds for skin tissue engineering applications for wound healing.


**Keywords:** Electrospinning; acetic acid; polymer-blend; fibroblasts; wound healing; tissue engineering.

## 1. Introduction

Blends of natural and synthetic polymers have gained increasing importance as biomaterials because they combine the properties of their constituents to result in materials with improved characteristics. Thus, hybrid blended scaffolds, composed of natural and synthetic polymers in different composition ratios, have been actively explored for different tissue engineering applications, such as skin, bone, cartilage, nerves or vessels (1–4). For skin tissue engineering, flexible scaffolds resembling the morphology and functionality of the extracellular matrix (ECM) constitute interesting materials that can provide support for cell adhesion, proliferation and differentiation, as well as wound cover (5–8). Hence, research has been focused on the development of mechanically-appropriate, natural-synthetic polymeric systems and fibrillar membranes capable of supporting and promoting fibroblasts (FB) adhesion and proliferation (9–15). Polycaprolactone (PCL) is a biocompatible, biodegradable, synthetic polymer approved by the U.S. Food and Drug Administration (FDA) for different medical applications (16). It has adequate structural and mechanical stability for soft-tissue engineering applications; however, its hydrophobic character limits its ability to promote cell adhesion and proliferation (17,18). On the other hand, gelatin (Gel) is a natural polymer derived from the partial hydrolysis of collagen, the major component of the ECM (19), that offers attractive biological advantages having the amino and carboxyl functional groups of collagen but displaying lower immunogenicity and antigenicity (20–22). Nevertheless, Gel rapid dissolution and weak mechanical stability in physiological conditions restricts its use for tissue engineering applications (18,23,24). One way to overcome the respective disadvantages of Gel and PCL is the use of Gel-PCL blends to develop biologically favorable and mechanically stable scaffolds for tissue engineering (10,11,22,25,26).

Low miscibility or immiscibility of natural and synthetic polymers usually limits the development of homogeneous blends of natural-synthetic polymers (27–31). The hydrophobic character of synthetic polymers such as PCL, polyacrylamide or poly(butylene succinate) normally induces hydrophilic natural polymers agglomeration during blending, resulting in phase-separated solutions (27,28). Phase separation is a manufacturing restriction for the fabrication of scaffolds by electrospinning, which is a technique commonly used in tissue engineering due to its ability to produce fibrillar mats that resemble the ECM morphology. Poorly blend solutions result in non-homogeneous electrospun fibers with a significant number of beads and discontinuities (26,28,32) that negatively impact the mechanical properties of the scaffolds (9,23) and their ability to promote cell adhesion and proliferation, e.g. for human keratinocytes and fibroblasts (22,33). Phase separation of natural-synthetic polymers blends is concentration dependent and normally worsens as the natural:synthetic polymers ratio increases, in contrast with the biologically favorable properties normally improving as this ratio increases (34,35). Therefore, it is necessary to overcome phase separation to produce homogeneous, natural-synthetic polymers scaffolds by electrospinning with adequate properties for skin tissue engineering applications.

Different solvents, such as dichloromethane, trifluoroethanol (TFE), chloroform, methanol or hexafluoro-2-propanol (HFP), have been used to improve the miscibility of Gel-PCL blends (11,32,36–38). In most reports, Gel-PCL solutions are produced in a three-step process where two independent solutions (for PCL and for Gel) are prepared and then mixed just before electrospinning. Commonly, at least two different solvents or mixtures of solvents are used to prepare the PCL and Gel solutions; nevertheless, HFP or TFE can be used as a common-solvent to obtain both solutions (38,39). For most traditional solvents or solvents mixture used for Gel-PCL electrospinning blends, for example,

chloroform/methanol-PCL and acetic acid-Gel solutions systems, critical phase separation occur at Gel concentration ≥ 20-30 wt.% (relative to total polymer weight) with severe phase separation at ≈ 50 wt.% Gel (32). On the other hand, fibroblasts adhesion and proliferation has been reported to significantly improve on PCL-Gel electrospun scaffolds with 30 wt.% Gel or higher (10,22,40). Recently, it was reported the incorporation of acetic acid (AcAc) as a dopant (0.2-0.3%) to TFE solutions of PCL or Gel to facilitate PCL-Gel miscibility, resulting in more homogeneous electrospun Gel-PCL scaffolds for up to 50 wt.% Gel (28). It was hypothesized that solution shift to pH = 4.7 (away from Gel isoelectric point, pH ≈ 5.0) caused by AcAc addition resulted in mutually exclusive positively charged Gel molecules with stretched chain configuration that facilitated penetration into PCL chains, improving the Gel-PCL miscibility (28).

Aqueous AcAc solutions can easily solubilize Gel due to its polar nature; in fact, Gel solutions in aqueous AcAc can be successfully electrospun into homogeneous Gel fibrillar scaffolds (18,21). Lately, it was shown by our group and other research groups that glacial AcAc solutions of PCL also present adequate properties for electrospinning, producing homogeneous fibrillar scaffolds (18,41,42). Thus, it can be expected that Gel-PCL homogeneous blends with Gel concentration ≥ 30 wt.% and appropriate electrospinning properties can be obtained in a straightforward single-step process by using AcAc as a sole solvent to dissolve PCL and Gel at once in a single solution. One advantage of this approach is that AcAc is a “green” solvent less toxic than other solvents, such as TFE or HFP commonly used for Gel-PCL electrospinning solutions (43). Furthermore, it is expected that the high acidity of AcAc (pH ≈ 2.4) used as a sole solvent can further protonate the amino groups of Gel molecules, in comparison to AcAc as a dopant with other solvents, further stretching the Gel chains and facilitating their interpenetration into the PCL chains to form miscible Gel-PCL blends. Another benefit of this AcAc sole solvent, single-step

approach is the ease of preparation; a single PCL-Gel-solvent mixing step is needed to obtain appropriate electrospinning solutions with high Gel concentration.

To the best of our knowledge, this is the first report using this AcAc sole solvent, single-step approach to obtain Gel-PCL blends suitable for electrospinning of homogeneous Gel-PCL scaffolds with Gel concentration ≥ 30 wt.%. In the present work, homogeneous Gel-PCL fibrillar scaffolds with 30 and 45 wt.% Gel were successfully electrospun using AcAc as a common single solvent for the Gel-PCL electrospinning solutions. The structural, chemical, thermal and mechanical properties of the scaffolds were evaluated, and their biological response was assessed *in vitro* using human FB as a model to evaluate their suitability for skin tissue engineering applications. Cell viability, metabolic activity and protein expression of tropoelastin and collagen Type I were studied.

## 2. Materials and Methods

### *2.1. Materials*

Glacial acetic acid (99.5%), hydrogen peroxide and Gelatin Type B derived from bovine skin were purchased from J.T Baker. Polycaprolactone (Mn = 80,000 Da), MTT ([3-(4,5-dimethylthiazol-2-yl)-2,5-diphenyltetrazolium bromide]), 2-propanol (99%), dimethyl sulfoxide (DMSO), copper(II) sulfate pentahydrate ($CuSO_4 \cdot 5H_2O$), potassium sodium tartrate ($KNaC_4H_4O_6 \cdot 4H_2O$), glutaraldehyde and diaminiobenzidine (DAB; DAKO K3468) were purchased from Sigma-Aldrich. Dulbecco's modified Eagle's medium (DMEM:F12), fetal bovine serum (FBS), penicillin/streptomycin (antibiotic/antimycotic) 0.25%, trypsin–EDTA 0.25%, phosphate buffered saline (PBS, pH = 7.4), Hank´s saline solution, dispase II and type I collagenase were acquired from GIBCO. LIVE/DEAD® Viability/Citotoxicity (Calcein-AM/Ethidium homodimer) kit for mammalian cells was obtained from Invitrogen™.

Immunocytochemistry assay was performed using the Vectastain ABC Kit from Vector Labs. Goat primary anti-human antibody to collagen α1 Type 1 (dilution 1:50; sc-25974) and goat primary anti-human antibody to tropoelastin and, to a lesser extent, to mature elastin (dilution 1:50; sc-17580) were purchased from Santa Cruz.

2.2. *Preparation of fibrillar scaffolds*

Electrospinning of scaffolds was performed using a horizontal equipment assembled in our laboratory, consisting of a syringe pump (NE-4000 2-channel, Pump Systems Inc.), a high voltage power supply (EH60P1.5 Glassman High Voltage Inc.) and a grounded aluminum collector plate. Gel-PCL single solutions for electrospinning were prepared at room temperature (RT; ≈ 18 – 20 °C) by dissolving PCL into AcAc (98.5% v/v) at a concentration of 19% w/v, based on our previous work to obtain homogeneous defect-free electrospun PCL fibers (44), and simultaneously adding the adequate amount of Gel to produce Gel-PCL solutions with 30 or 45 wt.% Gel, relative to total polymer content in solution. Gel concentrations were chosen aiming to obtain homogeneous electrospun scaffolds by the single-step AcAc solution process reported herein, with Gel concentrations within the range where significant phase separation has been observed for other solvents systems (25% ≤ Gel wt.% ≤ 50%, depending on the solvent system) (27,39,45) and where appropriate cell response has been observed (Gel wt.% ≥ 15%) (22,46,47). Only-PCL solutions (19% w/v) in AcAc were also prepared at RT (≈ 18 – 20 °C) and used as a control to study the influence of Gel concentration on the scaffold's properties. The only-PCL and Gel-PCL blends solutions were stirred at 300 rpm for 48 h at RT. Viscosity of solutions was measured in a viscometer (Brookfield LVDV-E15) equipped with a small sample adapter and their conductivity was measured in a JENWAY 3540 conductivity meter. Gel-PCL fibrillar scaffolds were

obtained by electrospinning at 14 kV with a needle-to-collector distance of 14 cm and Gel-PCL solution pumped through a 21 Gauge metal needle at 1 mL/h. Only-PCL scaffolds were electrospun using the same solution feed rate but increasing the needle-to-collector distance and the voltage to 18 cm and 18 kV, respectively. Electrospinning process was conducted at ambient conditions (temperature ≈ 20 – 21 °C and relative humidity ≈ 46 - 48%) during 40 minutes for either only-PCL or PCL-Gel blends. After electrospinning, the scaffolds were removed from the collector and sterilized under ultraviolet light (UV) for 15 min on each scaffold side. Scaffolds were named according to their composition and Gel wt.% as follows: "o-PCL" for only-PCL scaffolds and "30Gel/PCL" and "45Gel/PCL" for 30 and 45 wt.% Gel scaffolds, as reported in Table 1.

**Table 1.** Chemical composition, viscosity and conductivity of electrospinning solutions and nomenclature of electrospun scaffolds.

| Scaffold | Gel (wt.%)[a] | PCL (wt.%)[a] | Viscosity[b] (cps) | Conductivity[c] (µS/cm) |
|---|---|---|---|---|
| o-PCL | 0 | 100 | 4750 ± 39 | 0.26 ± 0.01 |
| 30Gel/PCL | 30 | 70 | 4139 ± 139 | 18.72 ± 0.28 |
| 45Gel/PCL | 45 | 55 | 3530 ± 50 | 32.29 ± 0.25 |

[a]Scaffolds chemical composition according to total polymer content (100 wt.%) in electrospinning solution. [b]Viscosity of polymers solutions used for electrospinning of scaffolds. [c]Conductivity of polymers solutions used for electrospinning of scaffolds.

### *2.3. Physical-chemical characterization of the scaffolds.*

#### *2.3.1. Morphology*

To characterize the overall macro and microscopical morphology and structure of the as-synthesized scaffolds, macroscopic photographs and light optical microscope photographs (micrographs; Axio Imager Z2, Carl Zeiss) of the scaffolds were acquired. Macroscopic photographs were acquired from

the same scaffolds samples (obtained from the central area of the electrospinning collector) as used for all experiments and measurements in the present study; however, micrographs were acquired from thinner scaffolds samples obtained from the edge areas of the electrospinning collector to allow light transmission through the scaffolds and appropriate micrographs acquisition. The thickness of 6 different samples for each different membrane was measured with a digital micrometer (Mitutoyo 293-140 QuantuMike). To characterize the precise scaffolds micro-morphology, samples were sputtered coated with carbon and observed with a JEOL-7600 Scanning Electron Microscope (SEM) using an accelerating voltage of 10.0 kV. Fiber diameter distribution was calculated by measuring (AxioVision software; Carl Zeiss Microscopy GmbH) the diameter of 80 fibers in total, proportionally selected from two different SEM micrographs acquired from the air and the collector sides of the scaffolds. Measurements from both scaffolds' sides micrographs were averaged as one group of measurements per scaffold. Average fiber diameter ± standard deviation (SD) is reported.

*2.3.2. IR Spectroscopy*

Chemical functional groups were analyzed by Infrared Spectroscopy. FTIR spectra were acquired by means of an infrared spectrometer (Nicolet 880 FTIR) with Attenuated Total Reflection (ATR) module at 4 $cm^{-1}$ resolution and 32 scans in a wavenumber range of 4000-400 $cm^{-1}$. Spectra of pristine Gel and PCL were acquired as reference for the assignment of the IR bands in the spectra of the as-electrospun o-PCL, 30Gel/PCL and 45Gel/PCL scaffolds. FTIR spectra of the scaffold samples, as used for the *in vitro* cells assays (i.e. scaffolds rinsed in water and ethanol, and left 48 h to dry at RT before UV-sterilization) were acquired before and after UV-sterilization to identify the possible UV-sterilization effects on the scaffolds components.

*2.3.3. Wettability and water contact angle*

Scaffolds hydrophilic/hydrophobic character was determined from WCA measurements performed in a video-enabled goniometer (OCA 15EC; Dataphysics) via the static sessile drop method using 4 µL double distilled water drops at RT. WCA were measured on dry and hydrated (in deionized water to their water uptake plateau; Supplementary Figure S1) scaffolds samples to assess a) their wettability over time and b) their stable WCA values discarding the influence of the water absorption effect, respectively. WCA were automatically calculated (156 frames/s) using the SCA20_U software over the whole time period of video recording; that is ≈ 5 s (until disappearing of water drop round shape on Gel-PCL blends scaffolds) or ≈ 10 s (until a stable WCA plateau was observed) for the dry and hydrated samples, respectively. WCA reported values represent the mean ± SD of three independent measurements for each different scaffold at different time points for dry samples or at the stable plateau for hydrated samples.

*2.3.4. Crystallinity*

XRD patterns of the scaffolds were acquired to characterize their crystalline or amorphous nature, which can be seen as an indication of the miscibility of the components in the Gel-PCL composite scaffolds. XRD patterns were acquired in a PANalytical X'Celerator diffractometer using CuKα radiation (λ = 1.54 Å; 40 mA, 40 kV) in Brag-Brettano configuration with 2Θ = 10 to 50°, step size of 0.05° and time/step of 20 s.

*2.3.5. Mechanical Properties*

Mechanical properties of the scaffolds were characterized using a mechanical uniaxial test equipment (AGS-X; Shimadzu) with 100 N load cell under cross-head speed of 1 mm/min at ambient conditions (≈

20 °C and 48% of relative humidity). Four specimens conforming the ASTM D1708-06a test specimen size (probes with free rectangular gauge length = 25 mm and width = 5 mm) for each different scaffold were hydrated in deionized water to their water uptake plateau (Supplementary Figure S1) and analyzed. Four dry specimens conforming the ASTM D1708-06a test specimen size for each different scaffold were also analyzed for comparison purposes. Samples thickness was measured with a digital micrometer (Mitutoyo 293-140 QuantuMike) in three different points of the gauge length. The stress-strain curves from raw load-displacement data were obtained and the elastic modulus (E), tensile strength (σ) and elongation at break (Ɛ) were determined from the stress-strain curves and are reported as the average results ± SD.

*2.3.6. Thermal properties*

Scaffolds thermal properties were investigated by means of TGA and DSC. TGA measurements were performed using a TGA2950 (TA Instruments) thermogravimetric analyzer with heating rate of 10 °C/min from room temperature to 700 °C under nitrogen atmosphere. DSC measurements were acquired using a Q2000 DSC equipment (TA Instruments). Thermal scans were acquired over a temperature range of -90 to 150 °C at heating rate of 10 °C/min in nitrogen atmosphere. Quench cooling was applied after first heating scan; then, a second heating scan was performed to erase the thermal history, and this was used to estimate the real thermal response of scaffolds. Scaffolds degree of crystallinity as percentage, $\chi_c$, was calculated from the melting peak ($T_m$) observed on the DSC thermograms according to Eq. 1 (48):

$$\chi_c = \left(\frac{\Delta H_m}{\Delta H_m^0}\right) \times 100 \qquad \text{(Eq. 1);}$$

where $\Delta H_m$ is the scaffolds sample melting enthalpy (endothermic peak related to the melting of PCL crystals) and $\Delta H^0_m$ is the reference melting enthalpy of 100% crystalline PCL; $\Delta H^0_m$ = 142.0 J/g (49,50). The observed $T_m$ on DSC thermograms can be ascribed only to the PCL component (the only scaffold component that can develop a crystalline phase due to its semi-crystalline structure) since the Gel component is totally amorphous and has not a specific melting peak associated. Data extracted from TGA and DSC studies were analyzed using the Universal Analysis® software.

*2.3.7. Gelatin Release*

Gelatin released from Gel-PCL scaffolds in aqueous solution was determined by the Biuret method (51). The Biuret reagent was prepared by dissolving 0.25 g of $CuSO_4 \cdot 5H_2O$ and 1.12 g of $KNaC_4H_4O_6 \cdot 4H_2O$ in 66.6 mL of distilled water. Then, upon constant stirring, 7 g of NaOH dissolved in 66.6 mL of distilled water was incorporated to the solution. Finally, 34.6 mL of distilled water was added, and the obtained stock Biuret solution was transferred to a light-protected bottle and stored at 4 °C. To establish the absorbance *vs* Gel concentration calibration curve, different standard solutions with Gel concentration of 0.2, 0.25, 0.5, 1.0, 1.5, 2.0, 2.5 and 5.0 mg/mL were prepared from a stock Gel:PBS solution (10 mg/mL). Aliquots of 0.5 mL of each standard solution, and of PBS to determine blank absorbance, were mixed with 2.25 mL of Biuret reagent. After 15 min of reaction at RT, solution absorbance was measured at 560 nm in a UV-Vis spectrophotometer (Cary 1E Varian). To determine the amount of Gel released from Gel-PCL scaffolds, samples (20 ± 0.94 g) of each scaffold were independently immersed in 2 mL of PBS and incubated at 37 °C in an orbital shaking incubator (mrclab TU400) at 80 rpm. After 1 day and then every three days up to 7 days, incubation medium was replaced for fresh medium, following the same medium change time schedule for the cellular tests of the scaffolds. 0.5 mL aliquots of the immersion supernatants, collected at every medium change time-

point, were mixed with 2.25 mL of stock Biuret solution, absorbance was read at 560 nm and Gel concentration in supernatants was obtained using the calibration curve. Finally, total amount of Gel released was calculated for each sample. Experiments were independently performed by triplicate. Results are presented as the average of Gel released from the scaffolds in percentage relative to theoretical (according to PCL:Gel ratio in electrospinning solution and scaffold samples weight) total Gel content in as-electrospun scaffolds.

*2.3.8. Degradation*

To evaluate scaffolds degradation, dry scaffolds samples (1.5 cm in diameter) were weighed ($W_0$) and incubated in 1 mL of PBS at 37 °C and 80 rpm; PBS was changed every day. At 1, 2, 3, 4, 5, 6, 7 and 17 days of incubation, samples were rinsed with distilled water, dried at 37 °C for 24 h and weighed ($W_1$). Evaluations from 1 to 7 days were set to properly asses the first fast but short degradation period expected for the composite scaffolds (mainly due to Gel loss). After that, a longer evaluation time point (17 days) was set to corroborate the slow degradation process expected to occur (due to PCL hydrolytic degradation) after the first fast degradation stage of the composite scaffolds. Weight loss ($W_{loss}$) in percentage was calculated at each testing time using Eq. 2:

$$W_{loss}(\%) = \left(\frac{W_0 - W_1}{W_0}\right) \times 100 \quad \text{(Eq. 2).}$$

*2.4. In vitro biological characterization of scaffolds.*

Human fibroblasts were isolated from scavenged skin specimens following circumcision surgeries of healthy pediatric patients, whose parents responded to an Informed Consent approved by the INR Institutional Research Ethics Committee (INR-11/12) (52). Specimens were washed in PBS with 10% v/v antibiotic-antimycotic, mechanically fragmented and incubated with dispase II (1 mg/mL). Then, the

epidermis was discarded, and the dermis was enzymatically digested in type 1 collagenase (0.3% solution). Finally, FB were collected by centrifugation and plated in culture flasks with DMEM:F12 supplemented with 1% v/v antibiotic-antimycotic and 10% v/v FBS (supplemented-DMEM:F12). Cell cultures were incubated in 5% $CO_2$ humidified atmosphere at 37 $^oC$ and culture medium was changed every two days. Confluent cell cultures were treated with 0.05% trypsin-EDTA, collected, plated and cultured in supplemented-DMEM:F12 for cells subcultures. FB were expanded until passage 3-5 when cells were collected and used for characterization of the biological response towards the scaffolds.

Scaffolds samples (diameter = 8 mm) for *in vitro* cell studies were rinsed in ethanol and water, dried and sterilized (UV light), and individually placed in 48-well culture plates by triplicate, seeded with 5 x $10^4$ cells suspended in 20 µL of supplemented-DMEM:F12 and incubated for 1 h at 37 °C and 5% $CO_2$. Then, fresh supplemented-DMEM:F12 was added to 200 µL per well. Samples were placed back in the incubator and cultured at 37 °C and 5% $CO_2$; culture medium was changed every 2 days.

Cell viability was evaluated at two different time intervals using the LIVE/DEAD assay kit (calcein AM/ethidium homodimer). After 1 and 3 days of culture, independent cell-cultured scaffolds were incubated with ethidium homodimer and calcein-AM in Hank's saline solution according to LIVE/DEAD assay kit manufacturer guidelines. Finally, samples were rinsed twice with PBS and visualized by Fluorescence Microscopy (Axio Imager Z2, Carl Zeiss). Images were processed using the AxioVision software® and cell viability (green/red; viable/dead cells) was qualitatively evaluated from micrographs.

Metabolic activity (as an indirect quantitative measurement of cell viability) of FB cultured on scaffold samples was determined using the colorimetric MTT-Formazan assay. After 1, 3 and 7 days of cell culture; independent cell-seeded and unseeded scaffold samples were rinsed twice with PBS,

placed in clean well plates and incubated with DMEM-F12:MTT solution (1:10) at 37 °C for 3 h. After MTT incubation, cell-metabolized formazan crystals were solubilized in 2-propanol:dimethyl sulfoxide (ISO:DMSO; 1:1) and solution absorbance was read at λ = 570 nm (Synergy HTX, Bio Tek instrument). A calibration curve was set to establish the number of metabolically active cells (number of cells) as a function of the absorbance reads from the MTT-formazan assay. For the calibration curve, a known number of cells (in a range from 10,000 to 120,000 cells with 6 intervals at different number of cells) was seeded by triplicate in independent tissue culture well plates (TCP) and cultured overnight with supplemented-DMEM:F12 at 37 °C and 5% $CO_2$. Then, cells were tested by the MTT assay, performed as previously described for the cells-seeded and unseeded scaffolds samples, and the number of cells seeded in the well plates was plotted against the absorbance reads.

Blank controls (unseeded scaffolds) absorbance reads were subtracted from the corresponding cells-seeded scaffolds absorbance reads to subtract the contributions of the possible MTT reagent absorption by the scaffolds themselves, and blank corrected absorbance values were transformed to number of cells on the scaffolds using the calibration curve. The number of cells on o-PCL scaffolds, at each MTT studied time period, was considered as the comparison control to evaluate the effect of Gel incorporation into the blend scaffolds on cell viability. All experiments were independently performed twice by triplicate for each incubation period evaluated (n=6).

To evaluate the adhesion and spreading of the fibroblasts on the scaffolds, after 1, 3 and 7 days of cell culture, independent cell-seeded scaffolds samples were fixed with glutaraldehyde, dehydrated in increasing concentration alcohol solutions and dried overnight at RT. Then, samples were sputtered coated with carbon and observed with a JEOL-7600 Scanning Electron Microscope using an accelerating voltage of 10.0 kV.

Immunocytochemistry assays were performed to identify the cell expression of tropoelastin (precursor of elastin) and collagen Type I, characteristics proteins of the dermis ECM. Three days after cell seeding on the scaffolds or on TCP (positive control, Ctrl+), samples were washed twice with PBS and fixed with PFA (2% in PBS). Fixed samples were permeabilized with Tween-20 (0.1%) and blocked with blocking serum (Vectastain ABC Kit). Then, independent samples were incubated overnight at 4 °C with primary antibodies to either against tropoelastin or collagen Type I (dilution 1:50 in PBS). After incubation, samples were rinsed three times with Tween-20 (0.1%) and incubated for 2 h at 37 °C with corresponding secondary antibody (Vectastain ABC Kit). Then, samples were rinsed three times with Tween-20 80.1%) and treated with DAB. Finally, cell nuclei were counterstained with Harris´s haematoxylin and micrographs were acquired by means of an optical microscope (Carl Zeiss). Immunocytochemistry negative controls (Ctrl-; no primary antibody used during the immunocytochemistry assay) were prepared of samples corresponding to cells incubated on the scaffolds and on TCP. To characterize the response of the scaffolds' materials per se to the immunocytochemistry assay compounds, unseeded scaffolds incubated in culture medium 3 days were also processed during the immunocytochemistry assay.

*2.5. Statistical analysis*

All results were plotted with Origin 9.0 Software. Statistical significance was determined by two-way analysis of variance (ANOVA), followed by a Tukey's multiple comparison test to compare pair groups. A value of $p < 0.05$ was considered statistically significant.

# 3. Results

*3.1. Conductivity and viscosity of electrospinning solutions*

The viscosity and conductivity of the o-PCL-AcAc, 30Gel/PCL-AcAc and 45Gel/PCL-AcAc solutions for electrospinning were assessed and the results are reported in Table 1. Viscosity of solutions significantly decreased with the addition of Gel to the solutions and it also significantly decreased with the increment of Gel concentration in the Gel-PCL blend solutions. Showing the opposite trend, the conductivity of the solutions significantly increased with the increment of Gel concentration in the electrospinning solutions.

*3.2. Physical-chemical properties of fibrillar scaffolds*

The overall macroscopic and optical microscopic aspect of the as-synthesized membranes is shown in Figure 1, from where it can be observed that the obtained scaffolds were flexible, resistant to the manipulation and characterized by a homogeneous fibrillar morphology. The average thickness of the scaffolds synthesized was 0.49 ± 0.04, 0.57 ± 0.04 and 0.81 ± 0.09 mm for o-PCL, 30Gel/PCL and 45Gel/PCL, respectively.

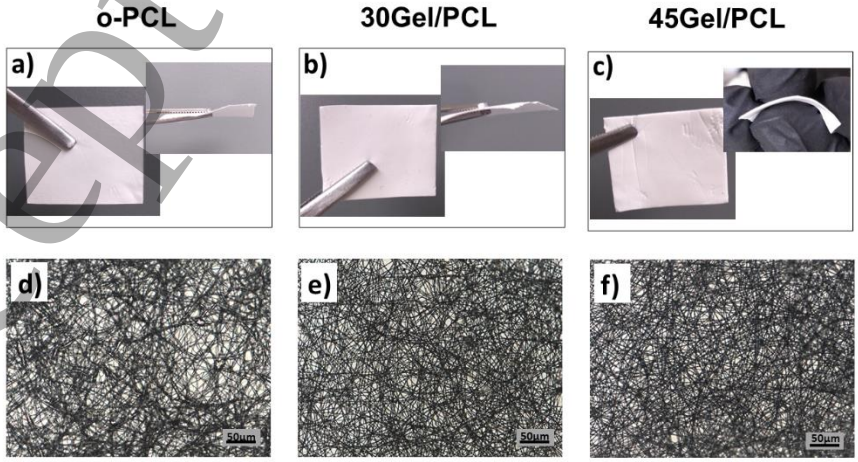

**Figure 1.** Representative (a-c) macroscopic photographs and (d-e) light optical microscope photographs (micrographs) of o-PCL, 30Gel/PCL and 45Gel/PCL scaffolds. Macroscopic photographs correspond to regular scaffolds samples (from the homogeneous central area of the electrospinning collector) used for all studies in the present work, while micrographs correspond to thinner scaffolds samples obtained from the edge areas of the electrospinning collector to allow light transmission through the samples and proper micrographs acquisition.

Representative SEM micrographs of o-PCL, 30Gel/PCL and 45Gel/PCL electrospun scaffolds are shown in Figure 2(a)-(c) along with the histograms of the scaffold's fibers diameter in Figure 2(d)-(f). Scaffolds exhibited fibrillar structures with randomly oriented fibers that were almost free of beads or defects. o-PCL scaffolds presented an average fiber diameter of 2.152 µm (Figure 2a and 1d). Addition of Gel to PCL electrospinning solutions resulted in narrower fibers. Average fiber diameter for 30Gel/PCL and 45Gel/PCL scaffolds was 0.755 and 0.708 µm, respectively (Figure 2e and 2f). Fibers diameter histograms showed narrower standard deviations for 30Gel/PCL (SD = 0.254 µm) and 45Gel/PCL (SD = 0.181 µm) than for o-PCL (SD = 0.756 µm). Average fiber diameter differences between o-PCL and either 30Gel/PCL or 45Gel/PCL were statistically significant at $p < 0.05$. However, differences between average fiber diameter between 30Gel/PCL or 45Gel/PCL were not statistically significant.

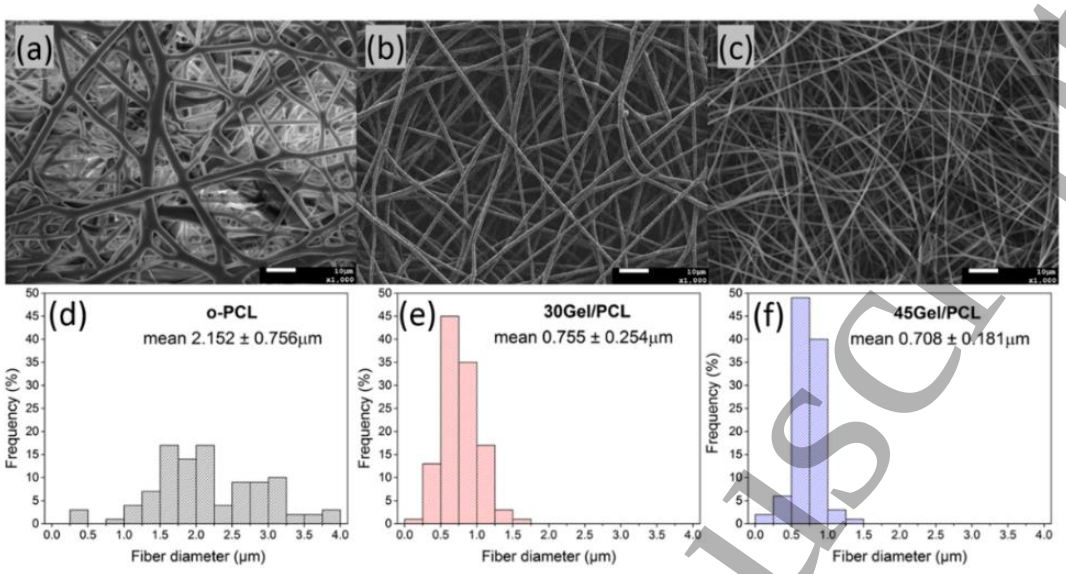


**Figure 2.** Representative SEM micrographs of a) o-PCL, b) 30Gel/PCL and c) 45Gel/PCL scaffolds, and the corresponding fiber diameter distribution histograms for d) o-PCL, e) 30Gel/PCL and f) 45Gel/PCL.

FT-IR spectra of pristine Gel, pristine PCL and as-electrospun o-PCL, 30Gel/PCL and 45Gel/PCL scaffolds are shown in Figure 3. The FT-IR spectra of 30Gel/PCL and 45Gel/PCL showed IR bands at wavenumbers below 3000 $cm^{-1}$ that were confidently assigned to either the PCL or Gel scaffolds' components (28,32,53,54) as indicated in Table 2. Nevertheless, the as-electrospun o-PCL scaffolds showed a new band at 3480 $cm^{-1}$ in comparison to pristine PCL, this band can be assigned to O-H stretching (28,53,54). On the other hand, the characteristic band of pristine Gel at 3296 $cm^{-1}$ (N-H stretching) was not clearly observed in the Gel-PCL scaffolds and instead, a broad band centered at ≈ 3296 $cm^{-1}$ was observed for the spectra of 30PCL/Gel and 45Gel/PCL. FTIR bands observed for pristine Gel, pristine PCL and o-PCL, 30Gel/PCL and 45Gel/PCL scaffolds and their corresponding vibrational assignment are listed in Table 2.

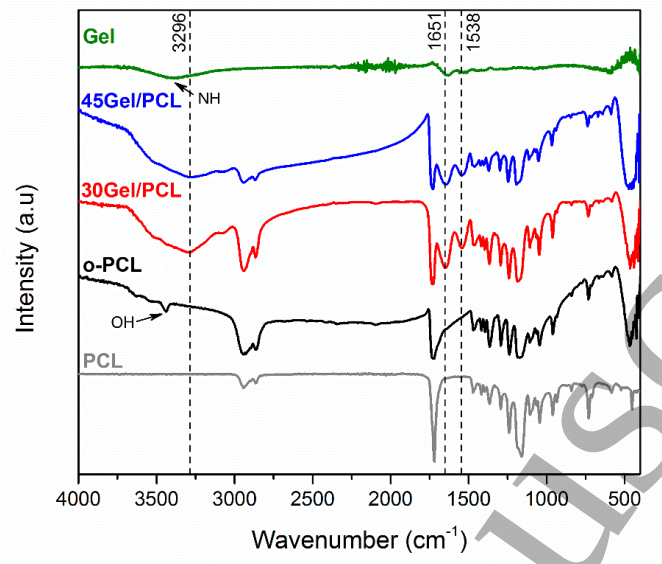


**Figure 3.** FTIR-spectra of pristine Gel, pristine PCL and as-electrospun o-PCL, 30Gel/PCL and 45Gel/PCL scaffolds. IR bands assigned to overlapping of O-H and N-H stretching (3296 $cm^{-1}$), C=O stretching amide I (1651 $cm^{-1}$) and N-H bending amide II (1538 $cm^{-1}$) are marked with black dotted lines.

**Table 2.** FT-IR bands observed for pristine Gel, pristine PCL and o-PCL, 30Gel/PCL and 45Gel/PCL electrospun scaffolds and their corresponding vibrational assignments.

| Wavenumber ($cm^{-1}$) | | | | Assignment | Reference |
|---|---|---|---|---|---|
| **PCL** | **Gel** | **o-PCL** | **Gel/PCL[a]** | | |
| | | 3488 | | O-H groups | (53) |
| | 3438 | | | N-H stretching amide bond | (28,53) |
| | | | 3296 | overlapping of O-H and N-H stretching | (54) |
| 2945 | | 2945 | 2945 | asymmetric $CH_2$ stretching | (32,53) |
| 2859 | | 2859 | 2859 | symmetric $CH_2$ stretching | (32,53) |
| 1731 | | 1731 | 1731 | C=O stretching | (32,53) |
| | 1651 | | 1651 | C=O stretching, amide I | (32,53,54) |
| | 1538 | | 1538 | N-H bending, amide II | (32,53,54) |
| 1294 | | 1294 | 1294 | C-C stretching | (32,53) |
| 1240 | | 1240 | 1240 | asymmetric C-O-C stretching | (32,53) |
| 1175 | | 1175 | 1175 | symmetric C-O-C stretching | (53) |
| 1045 | | 1045 | 1045 | C-O stretching | (32) |

[a]30Gel/PCL and 45Gel/PCL scaffolds showed the same IR bands and thus, they are included within the same column as Gel/PCL scaffolds.

The scaffolds were washed, and UV-sterilized before their use in the *in vitro* cellular assays. Then, dry washed scaffolds samples were assessed by FTIR spectroscopy before and after the UV-sterilization process (Figure 4) to assess the possible changes in the scaffolds chemical structure due to the UV-sterilization process; mainly the potential Gel crosslinking effects induced by the UV radiation. No evident shifts of the FTIR bands were observed before and after UV-sterilizations. Neither evident changes in the relative intensities or broadening of the IR bands in the spectra were observed. It is important to mention that in comparison with the as-electrospun scaffolds (Figure 3) the OH-stretching band (3488 $cm^{-1}$) observed for the as-electrospun o-PCL scaffold was not observed in the washed and/or not UV-sterilized scaffolds.

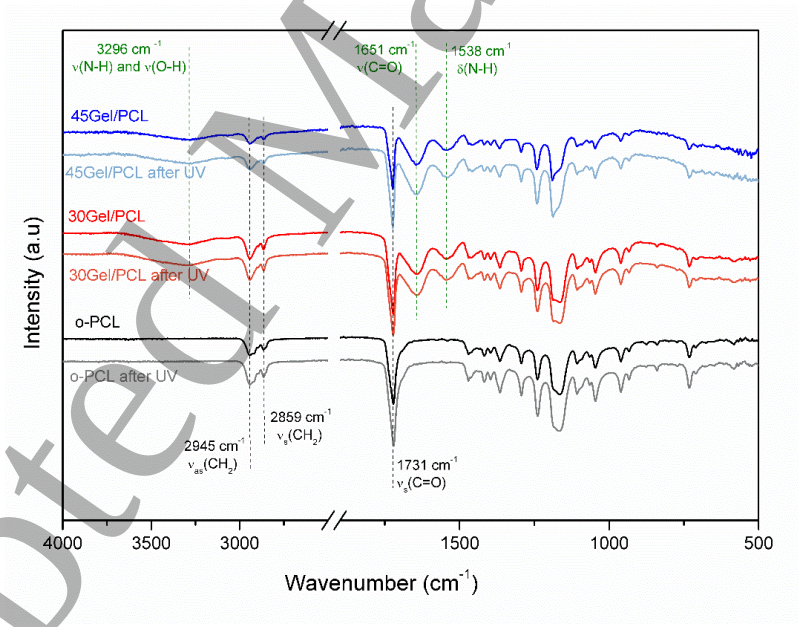


**Figure 4.** FTIR spectra of o-PCL, 30Gel/PCL and 45Gel/PCL scaffolds, as used for the *in vitro* cellular assays, before and after UV sterilization. Main bands corresponding to the expected characteristic IR bands from the Gel (dotted green lines) and PCL (dotted black lines) components in the scaffolds are marked.

Results of WCA measurements on dry samples at 1, 3 and 5 s and on hydrated samples at 10 s after water droplet deposition on the scaffolds are shown in Figure 5a and 5b, respectively. Droplets remained with semi-spherical shapes on dry o-PCL after 5 s of water droplet contact with the surface, exhibiting a stable WCA ≈ 131°. In contrast, water droplets on dry 30Gel/PCL and 45Gel/PCL quickly wetted the surface after first contact, WCA on initially dry Gel-PCL scaffolds quickly decreased from 66° (30Gel/PCL) and 56° (45Gel/PCL), immediately after water droplet deposition, to 34° (30Gel/PCL) and 14° (45Gel/PCL) after 5 s of water droplet deposition on the surface. On the other hand, on initially hydrated samples, the average WCA at the stable plateau for o-PCL scaffolds was 126° exhibiting a hydrophobic surface, while the stable average WCA on initially hydrated 30Gel/PCL and 45Gel/PCL samples was 65.1° and 25.3°, respectively, exhibiting that Gel-PCL blend scaffolds possessed a hydrophilic surface.

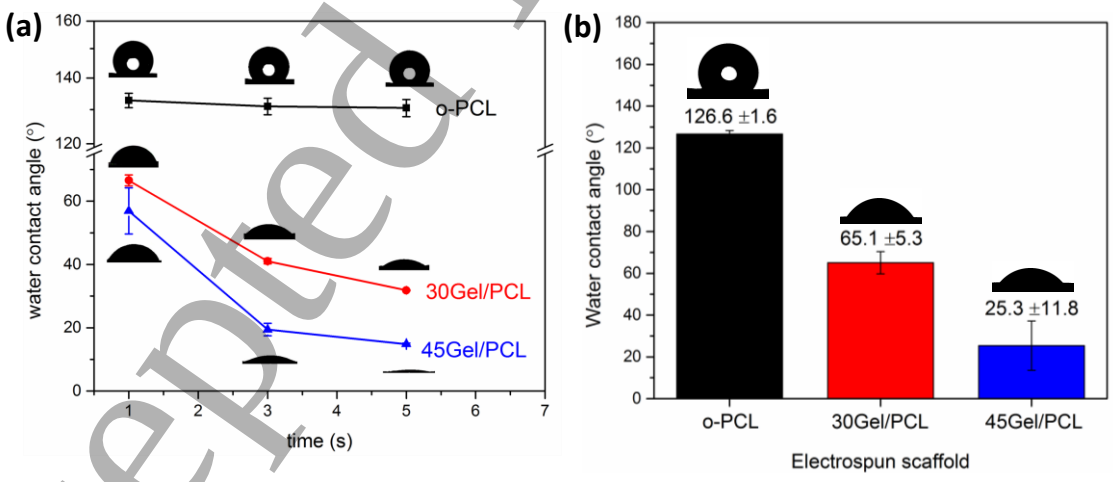


**Figure 5.** a) Water contact angles measured at 1, 2, and 5 s after water droplet deposition on initially dry samples of o-PCL, 30Gel/PCL and 45Gel/PCL scaffolds. b) Average stable water contact angles measured at 10 s after water droplet deposition on initially hydrated samples of o-PCL, 30Gel/PCL and 45Gel/PCL scaffolds.

Figure 6 shows the tensile mechanical parameters of hydrated o-PCL, 30Gel/PCL and 45Gel/PCL scaffolds; that is, their elastic modulus, E; maximum tensile strength, $\sigma_{max}$; and elongation at break, ε. Elastic modulus was 4.07 ± 1.46 MPa, 6.01 ± 0.61 MPa and 7.23 ± 2.11 MPa for o-PCL, 30Gel/PCL and 45Gel/PCL, respectively. Even when Gel addition to the scaffolds seemed to slightly increased the average elastic modulus of Gel/PCL scaffolds in comparison to o-PCL, the differences observed among the E values of the different scaffolds were not statistically significant ($p < 0.05$), and thus, the three different scaffolds studied in the present work, o-PCL, 30Gel/PCl and 45Gel/PCL, had similar elastic modulus in the hydrated state. The maximum tensile strength was also statistically comparable between the different scaffolds with o-PCL presenting a slightly higher maximum tensile strength in comparison to 30Gel/PCL and 45Gel/PCL but with no statistical significance for the differences observed; $\sigma_{max}$ was 1.21 ± 0.35 MPa, 0.96 ± 0.03 MPa and 1.03 ± 0.08 MPa for o-PCL, 30Gel/PCL and 45Gel/PCL, respectively. On the other hand, the elongation at break of the scaffolds with Gel, 30Gel/PCL and 45Gel/PCL, was ≈ 51% higher than that of the o-PCL scaffolds with a statistical significance for the differences observed between the elongation at break of o-PCL and that of the Gel/PCL scaffolds; nevertheless, no significant differences in the elongation at break between the 30Gel/PCL and 45Gel/PCL scaffolds were observed (ε ≈ 144% for both scaffolds). Tensile properties of dry scaffolds samples (Supplementary Figure S2) evidenced a significant change (increase) only for the maximum elongation at break of dry o-PCL (E = 6.09 ± 3.10 MPa, $\sigma_{max}$ = 2.27 ± 0.94 MPa and ε = 238.25 ± 59.12%) in comparison to hydrated o-PCL. However, 30Gel/PCL and 45Gel/PCL scaffolds showed a significant different mechanical behavior in the dry and hydrated states, with stiff and brittle characteristics in the dry state (Supplementary Figure 2; E = 12.66 and 49.56 MPa, $\sigma_{max}$ = 1.46 and 0.66

MPa and ε = 62.67% and 1.53% for dry 30Gel/PCL and 45Gel/PCL, respectively) and plastic properties in the hydrated state (Figure 6).

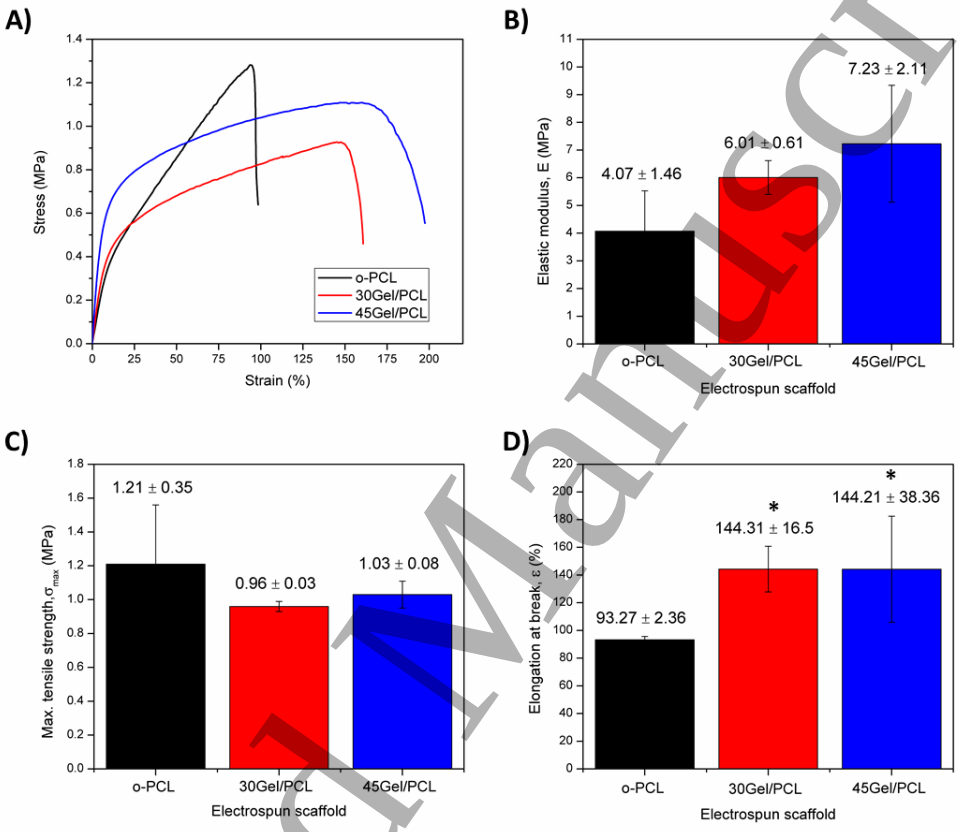


**Figure 6**. Mechanical tensile parameters of the scaffolds calculated from hydrated scaffolds samples: (A) representative strain vs stress curves; (B) elastic modulus, E; (C) maximum tensile strength, $\sigma_{max}$; and (D) elongation at break, Ɛ. *, $p < 0.05$ respect to o-PCL.

XRD patterns of o-PCL, 30Gel/PCL and 45Gel/PCL are shown in Figure 7. XRD patterns for o-PCL showed two strong diffraction peaks at 2Θ = 21.11° and 23.99° corresponding to the (110) and (200) planes of the semi-crystalline PCL structure, in agreement with literature (55). XRD patterns of

30Gel/PCL and 45Gel/PCL also showed the characteristic diffraction peaks of semi-crystalline PCL (Figure 7a) but with a smaller intensity; intensity of peak at 2Θ = 21.11° decreased 11.33% and 34.69%, respectively for 30Gel/PCL and 45Gel/PCL, in comparison to the corresponding peak for o-PCL (Figure 7b). No noteworthy diffraction peaks from Gel were observed for either 30Gel/PCL or 45Gel/PCL since Gel is fully amorphous.

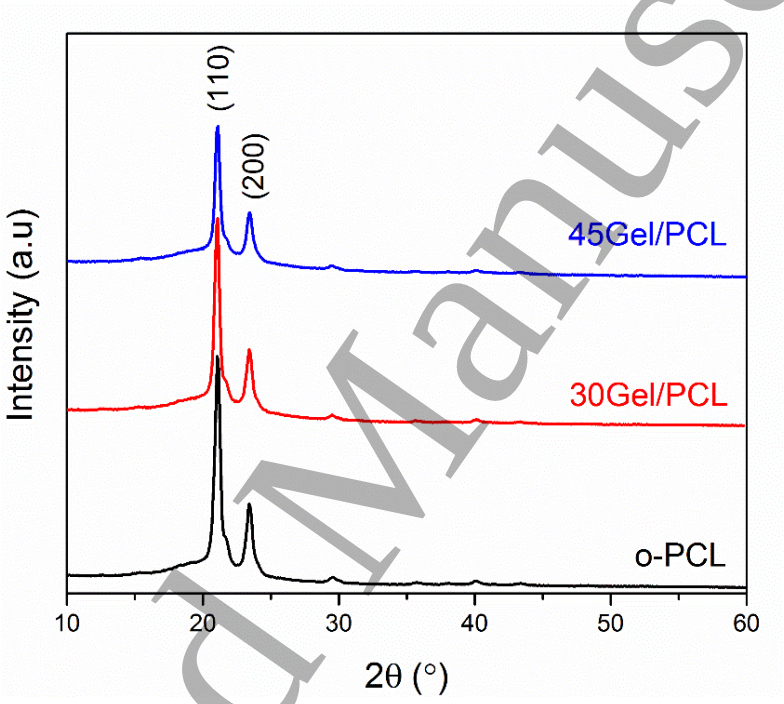


**Figure 7.** (a) XRD patterns of o-PCL, 30Gel/PCL and 45Gel/PCL scaffolds exhibiting diffraction peaks at 2Θ of 21.11° and 23.99°. (b) Enlarged region of the XRD patterns (2Θ from 19° to 25°) of o-PCL (black), 30Gel/PCL (red) and 45Gel/PCL (blue).

TGA curves of pristine Gel and o-PCL, 30Gel/PCL and 45Gel/PCL scaffolds are shown in Figure 8a, whereas data are summarized in Table 3. o-PCL showed a single weight loss step at a temperature of maximum weight loss rate ($T_{max}$) of 394 °C. Pristine Gel showed a first weight loss step at $T_{max}$ of 67°C that was attributed to water content, followed by a broad degradation step, where two weight

loss peaks can be identified at $T_{max}$ of 288°C and 317°C. Gel-PCL blended scaffolds (30Gel/PCL and 45Gel/PCL) also exhibited an initial weight loss due to water adsorbed mainly in the Gel component (35°C and 32°C) and weight loss peaks attributed to both components PCL (389°C and 387°C) and Gel (290°C, 324°C and 287°C, 318°C) with intensities that were correlated with the Gel:PCL ratio on the blend composition; that is, intensity of weight loss peaks attributed to PCL decreased as Gel:PCL ratio increased, while intensity weight loss peaks attributed to Gel increased as Gel:PCL ratio increased.

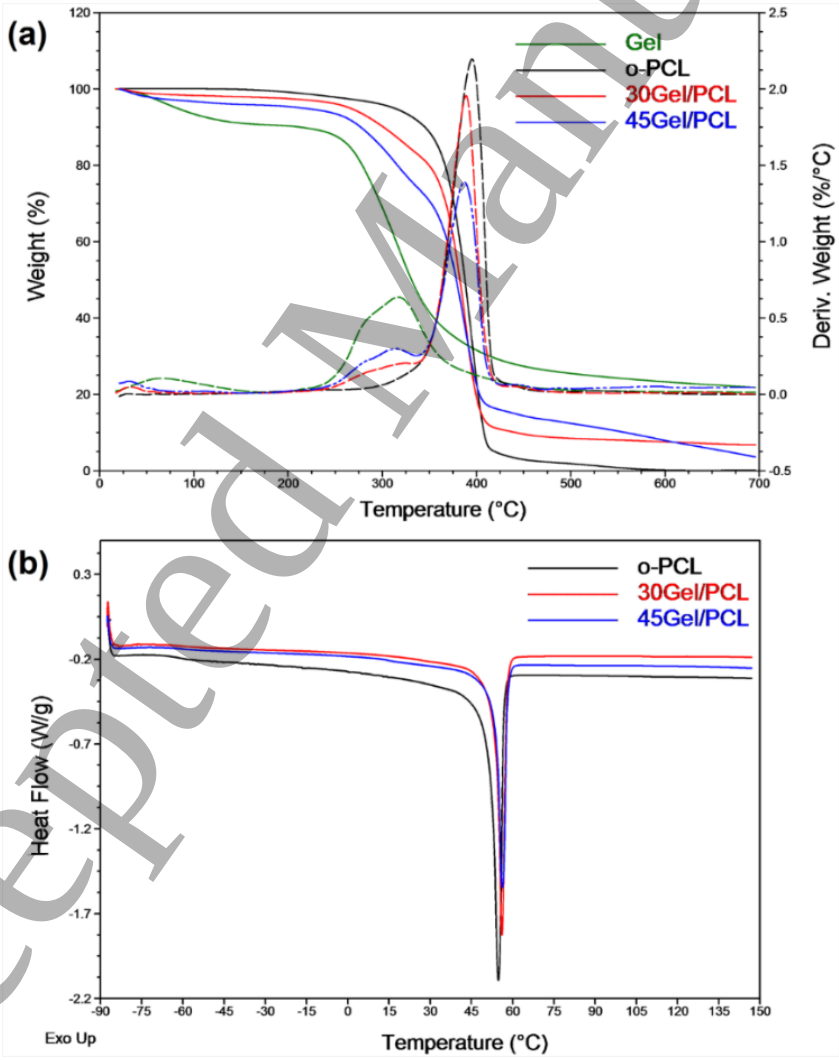

**Figure 8.** (a) TGA thermograms (solid lines) and derivative curves of weight loss (dotted lines) for pristine Gel, o-PCL, 30Gel/PCL and 45Gel/PCL scaffolds. (b) Heating DSC scans of o-PCL (black), 30Gel/PCL (red) and 45Gel/PCL (blue) scaffolds, after controlled cooling (10°C/min) from the melt.

**Table 3.** Thermogravimetric characterization of pristine Gel and o-PCL, 30Gel/PCL and 45Gel/PCL electrospun scaffolds.

| Material | Main region of thermal decomposition | | | | | |
|---|---|---|---|---|---|---|
| | Temperature range (°C) | Weight loss (%) | $T_{max}$ [a] (°C) | | | |
| Pristine Gel | 193 - 495 | 75 | 67 | 288 | 317 | - |
| o-PCL | 299 - 463 | 97 | - | - | - | 394 |
| 30Gel/PCL | 249 - 475 | 91 | 35 | 290 | 324 | 389 |
| 45Gel/PCL | 238 - 473 | 95 | 32 | 287 | 318 | 387 |

[a] Tmax is the temperature of maximum weight loss rate for each degradation step

Heating DSC scans of o-PCL, 30Gel/PCL and 45Gel/PCL are shown in Figure 8b and thermal properties are summarized in Table 4. A unique endothermal peak was detected in the heating scans for the three scaffolds; this peak was attributed to melting of the PCL component at a melting temperature ($T_m$) of about 55 °C. Scaffolds endothermic melting enthalpy ($\Delta H_m$) decreased as their Gel concentration increased, indicating that scaffolds $\chi_c$ decreased with increasing Gel concentration. The presence of the amorphous Gel component in the Gel-PCL blends scaffolds may either simply "dilute" the crystalline phase (due to the presence of the semi-crystalline PCL) or to some extent it could also inhibit the PCL crystallization. In order to answer this question, the melting enthalpy per gram of PCL present (according to the theoretical PCL-Gel composition of the scaffolds from Gel-PCL electrospinning solutions) in each blend scaffold ($\Delta Hm[PCL]$) was calculated (Table 4). The values

obtained were practically constant with a value at around 70 J/g, showing that, although the overall crystallinity degree of the blends decreased from o-PCL to 30Gel/PCL to 45Gel/PCL, the ability for crystallization of the PCL remained unaltered.

**Table 4.** Calorimetric properties of o-PCL, 30Gel/PCL and 45Gel/PCL electrospun scaffolds

| Scaffold | $T_m$[a] (°C) | $\Delta H_m$[b] (J/g) | $\Delta H_m$[PCL][c] (J/g) | $\chi_c$[d] (%) |
|---|---|---|---|---|
| o-PCL | 54 | 70 | 70 | 49 |
| 30Gel/PCL | 56 | 50 | 71 | 35 |
| 45Gel/PCL | 56 | 41 | 74 | 29 |

[a]melting temperature; [b]melting enthalpy; [c]melting enthalpy per gram of PCL; [d]$\chi_c$ = degree of crystallinity from melting enthalpy.

Figure 9a shows percentage of Gel released relative to the theoretical total Gel content of the scaffolds (calculated from the PCL:Gel ratio used in the electrospinning solutions) for 30Gel/PCL and 45Gel/PCL scaffolds incubated in PBS. After 1 d of incubation, 30Gel/PCL and 45Gel/PCL released ≈ 66% and ≈ 75% of their theoretical content of Gel, respectively. After 48 h of incubation, Gel released was ≈ 80% and ≈ 88% of their theoretical content of Gel for 30Gel/PCL and 45Gel/PCL, respectively. After 72 h, Gel released in PBS was ≈ 86% and ≈ 95% of the theoretical Gel content for 30Gel/PCL and 45Gel/PCL, respectively. At 5 and 7 days, no Gel content in the supernatants could be detected, within the resolution of the Biuret assay used in the present work.

Overall degradation behavior of o-PCL and Gel-PCL scaffolds in PBS (in terms of $W_{loss}$ in percentage as a function of time) is shown in Figure 9b. As expected, o-PCL did not show an important $W_{loss}$ ($W_{loss}$ < 4%) even after 17 days of incubation. After 3 days of incubation, Gel-PCL scaffolds

showed $W_{loss}$ equal to ≈ 26% and ≈ 43%, respectively for 30Gel/PCL and 45Gel/PCL. By day 17, 30Gel/PCL and 45Gel/PCL scaffolds evidenced a weight lost (≈ 28% and ≈ 44 %, respectively for 30Gel/PCL and 45Gel/PCL) very similar to that observed since day 3 of the degradation test.

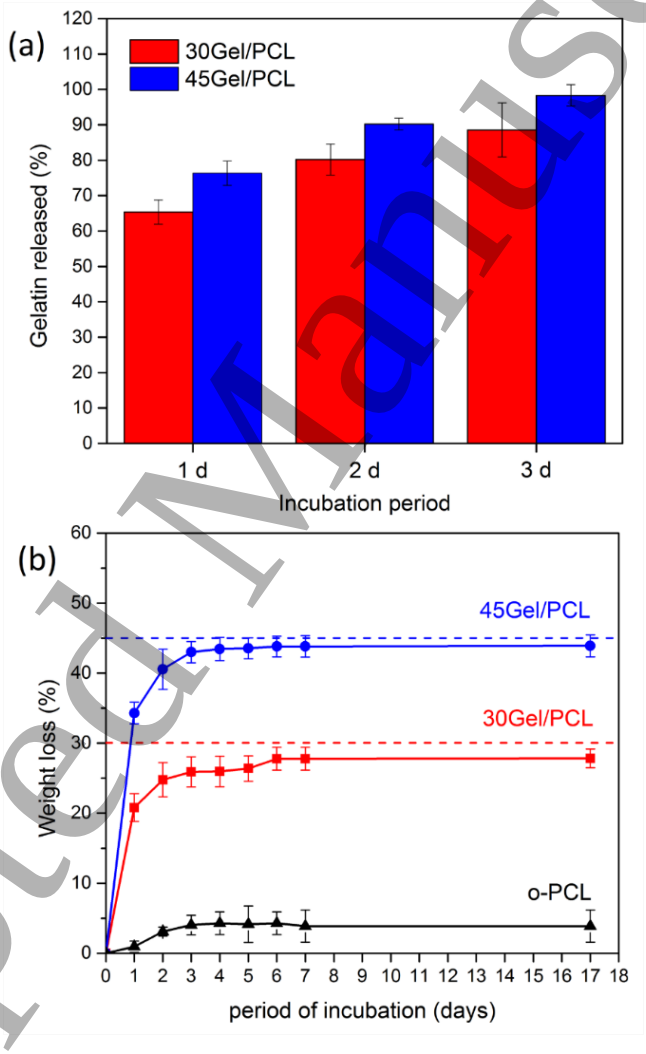


**Figure 9.** (a) Percentage of gelatin released (relative to theoretical gelatin content of the scaffolds, according to the electrospinning solutions prepared) in PBS from 30Gel/PCL and 45Gel/PCL scaffolds as determined by Biuret assay. (b) Weight loss percentage over time of o-PCL, 30Gel/PCL and 45Gel/PCL scaffolds incubated in PBS; dotted lines indicate the theoretical gelatin content in wt.% of the Gel/PCL scaffolds (accordingly to the composition of the electrospinning solutions prepared).

3.2. *In vitro biocompatibility of the scaffolds.*

The number of (metabolically active) cells on Gel-PCL scaffolds after 1, 3 and 7 days of culture is shown in Figure 10. The number of viable cells on the scaffolds was indirectly evaluated by the MTT-Formazan assays using a calibration curve to obtain the number of cells (metabolically active) on the scaffolds from MTT-Formazan assay absorbance reads.

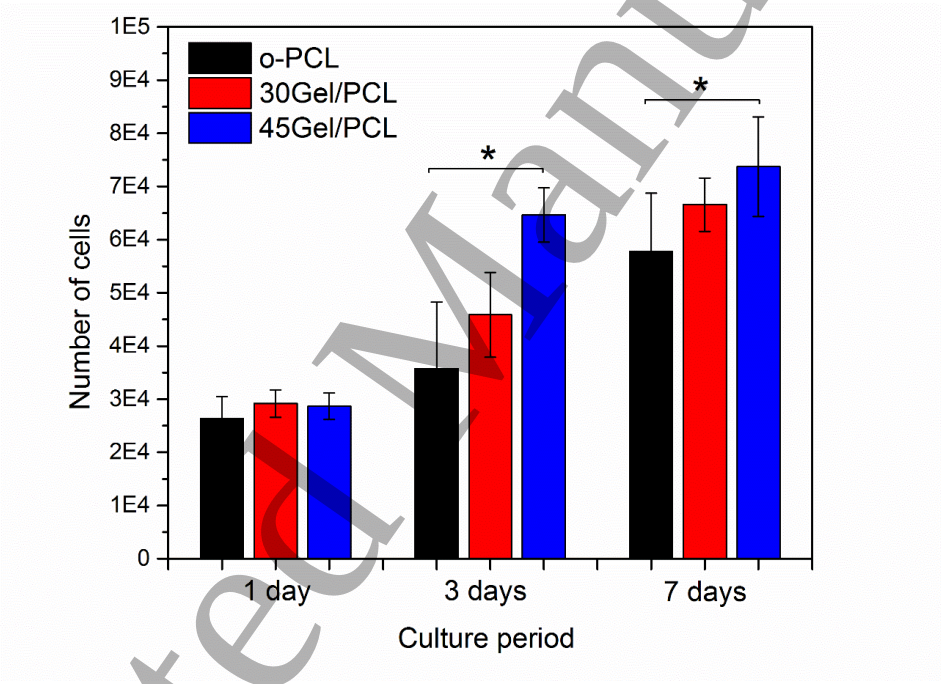


**Figure 10.** Number of cells (metabolically active) on the scaffolds calculated from the MTT-Formazan assay performed on fibroblast cultured on o-PCL, 30Gel/PCL and 45Ge/PCL at three different cell culture periods, 1, 3 and 7 days. *, $p < 0.05$ vs. o-PCL at corresponding cell culture time.

Number of cells on the scaffolds increased with culture days. The number of cells on the Gel-PCL scaffolds was larger than that on the o-PCL scaffold at each corresponding evaluation time point.

However, only the number of cells on 45Gel/PCL at 3 and 7 days of cell culture was significantly larger than the number of cells on the o-PCL scaffold at the corresponding incubation time. Cell metabolism can be seen as an indirect measurement of cell viability (number of metabolically active cells) on the scaffolds and thus, it is possible to state that cell viability increased for the blend scaffold 45Gel/PCL in comparison to o-PCL.

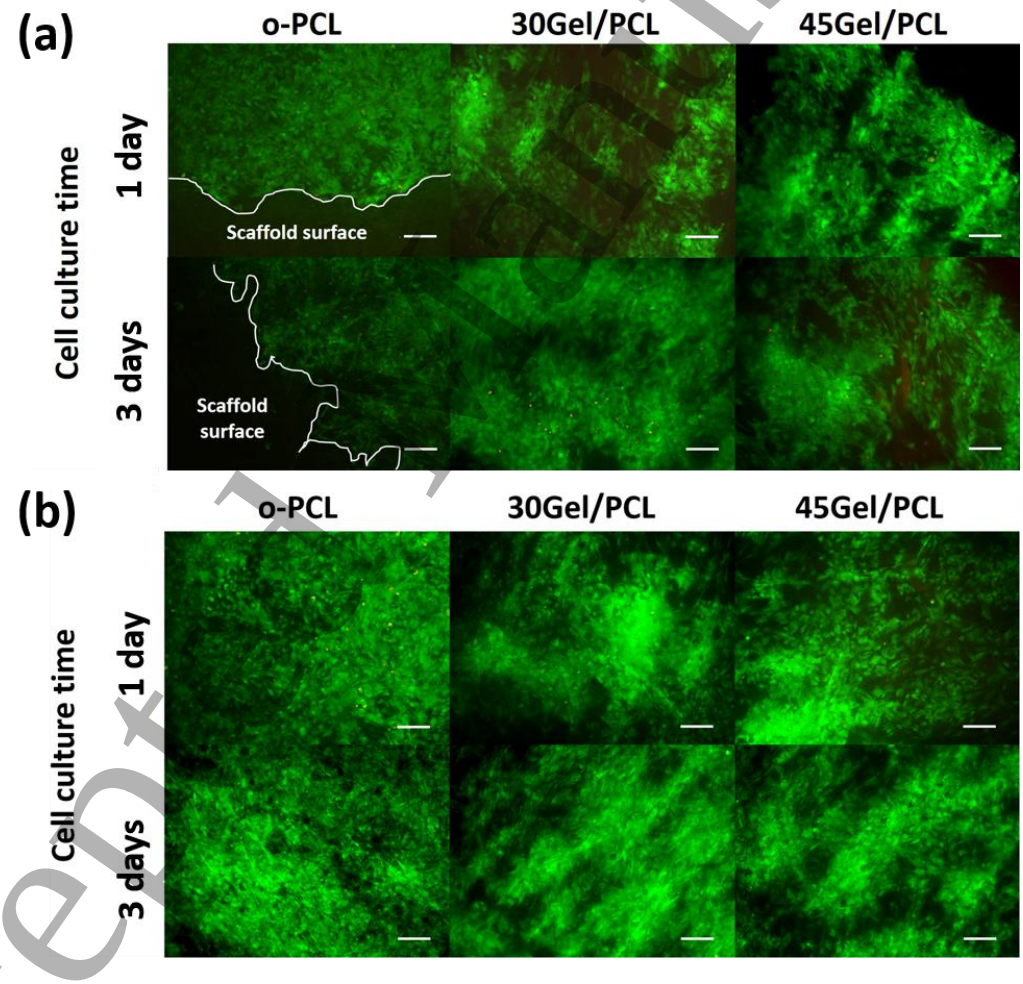


**Figure 11.** Representative fluorescence micrographs of the a) border and b) central areas of the scaffolds from LIVE/DEAD assay on fibroblasts cultured for 1 and 3 days on o-PCL, 30Gel/PCL and 45Ge/PCL scaffolds. Scale bar corresponds to 100 µm. Alive and dead cells are observed in green and red, respectively.

Representative fluorescence micrographs of the border and central areas of the scaffolds acquired from LIVE/DEAD (calcein/ethidium homodimer) assay after 1 and 3 days of cell culture on o-PCL and Gel-PCL scaffolds are shown in Figure 11. From qualitative analysis of the micrographs, it can be observed a high percentage of cell viability (green; alive cells) with few dead cells (red) on the three different scaffolds studied. The same results were observed at the two different culture intervals tested in the present study. Nevertheless, it is important to emphasize that cells mainly remained within the central area of the scaffold where they were originally drop-seeded for the o-PCL scaffolds (Figure 11B), leaving the border areas of the o-PCL scaffolds uncovered even after 3 days of culture (Figure 11A). On the other hand, cells cultured on the 30Gel/PCL and 45Gel/PCL scaffolds homogeneously spread over the whole surface of the scaffolds (remaining at the central area of the scaffolds where cells were originally seeded and conquering also the border areas of the scaffolds), covering the entire available area of the Gel-PCL blend scaffolds surface (Figure 11 A-B) after 3 days of cell culture.

Representative SEM micrographs of cells seeded o-PCL, 35Gel/PCL and 45Gel/PCL scaffolds samples cultured for 1, 3 and 7 days are shown in Figure 12. From these micrographs it can be observed that cells were well-adhered on all the scaffolds after 1 day of incubation. With increasing culture time, cells conquered the surface of the scaffolds and seemed to remain well adhered with a significant amount of extracellular matrix deposited. Although cells are well adhered and extended over the surface of all the scaffolds, cells on Gel-PCL blend scaffolds seemed to present a more homogeneous coverage of the surface of the scaffolds in comparison to cells on o-PCL. By 7 days of

culture on 30Gel/PCL and 45Gel/PCL, cells covered the whole surface of the scaffolds (mainly cells on 30Gel/PCL) forming a homogeneous and dense layer of well-adhered cells.

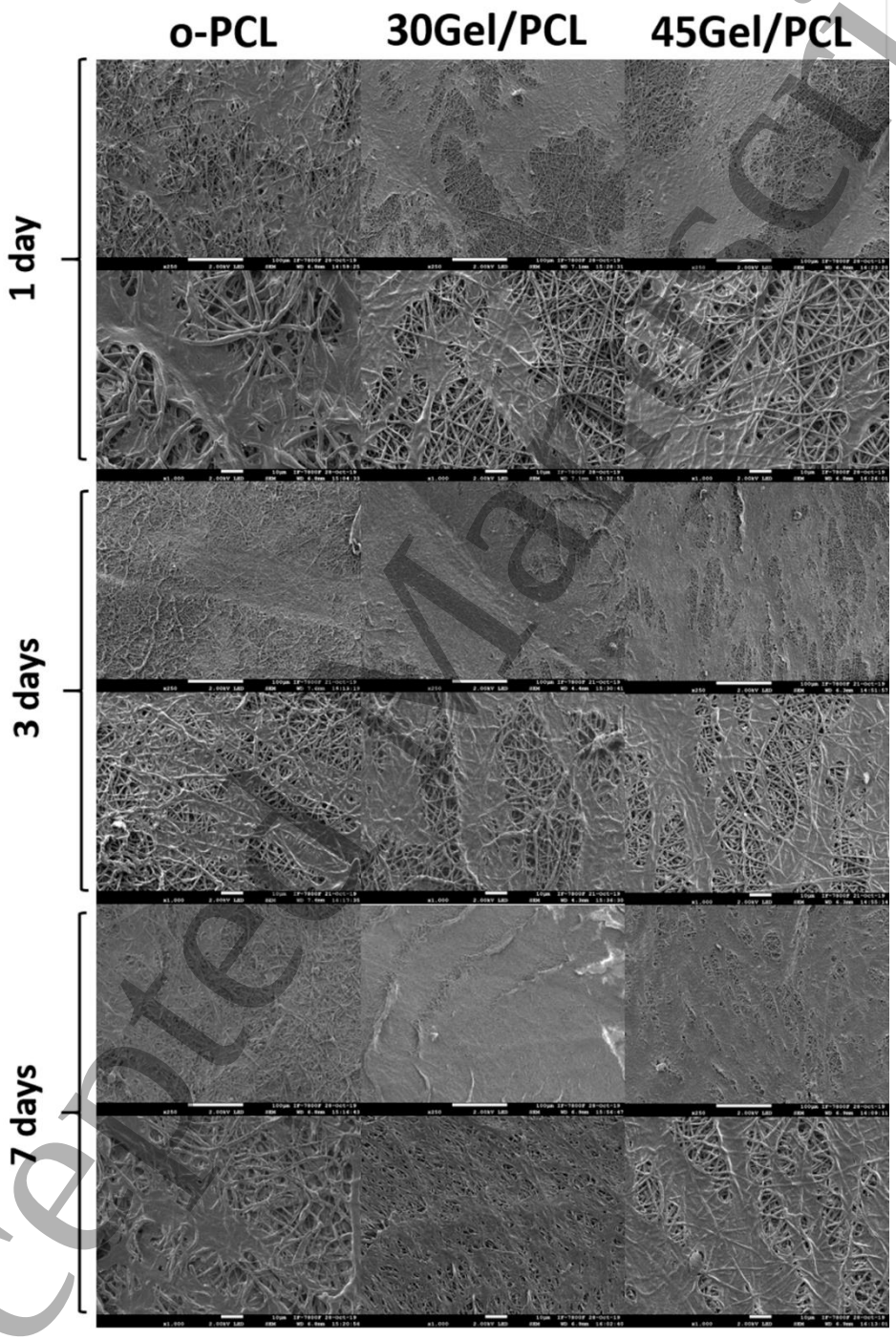


**Figure 12.** Representative micrographs of cells on o-PCL, 35Gel/PCL and 45Gel/PCL scaffolds samples after 1, 3 and 7 days of culture.

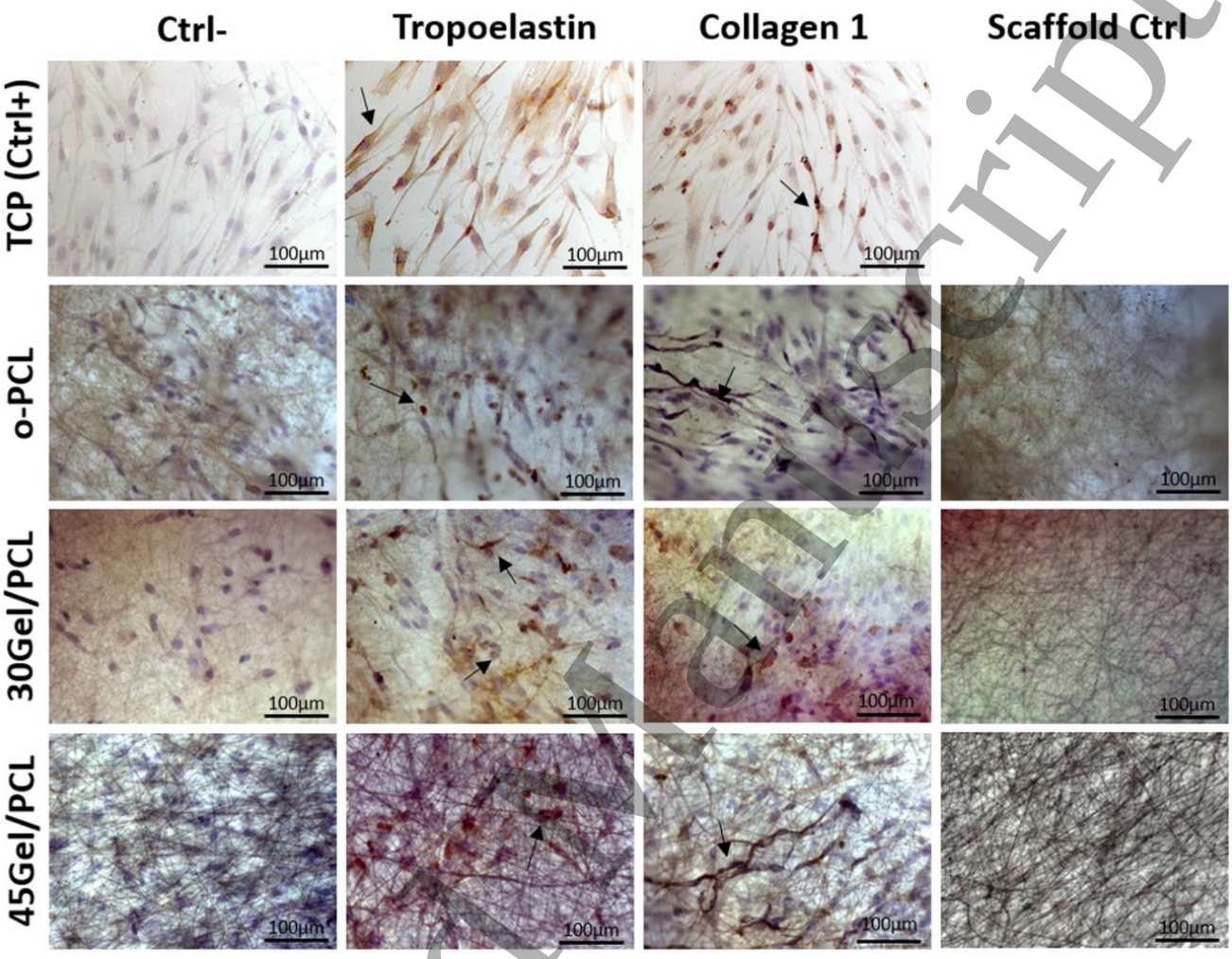


**Figure 13.** Representative immunocytochemistry micrographs after 3 days of cell culture on o-PCL, 30Gel/PCL and 45Gel/PCL scaffolds and tissue culture well plates (TCP positive control; Ctrl+). Positive staining to tropoelastin and collagen Type I is observed in deep brown (black arrows). Ctrl- correspond to immunocytochemistry assay negative controls (no primary antibody). Scaffold Ctrl correspond to immunocytochemistry assays on unseeded scaffolds. Scale bar corresponds to 100 µm.

Expression of characteristic fibroblasts proteins from cells seeded on o-PCL and Gel-PCL scaffolds was analyzed by immunostaining of tropoelastin and collagen Type I, characteristic proteins of dermis ECM. Representative immunocytochemistry micrographs after three days of cell culture on

the scaffolds or on TCP (Ctrl+) are shown in Figure 13. Immunocytochemistry negative controls (Ctrl-) did not present brown color staining around the blue cell nuclei for neither cells culture on TCP, o-PCL or Gel/PCL scaffolds, corroborating the specificity of the immunocytochemistry assay. Controls (Scaffolds Ctrl-) to assess the potential interaction of the immunocytochemistry assay compounds with the components of the scaffolds (mainly with gelatin) were also performed by studying unseeded (but culture in culture medium) scaffolds by immunocytochemistry.

From Figure 13, it can be observed that FB cultured on o-PCL and Gel/PCL scaffolds expressed tropoelastin and collagen Type I (zones of deep brown staining around cells blue nuclei marked with black arrows in Figure 13). Expression of both proteins by cells cultured on the scaffolds was similar to that of the Ctrl+ (cells on TCP). It is important to mention that fibers of the scaffolds presented a slight unspecific brown staining upon immunocytochemistry assays (Figure 13; Scaffolds Ctrl column), mainly 45Gel/PCL; however, this unspecific staining did not prevent distinguishing cell positive expression of tropoelastin or collagen Type I (deep brown staining; black arrows in Figure 13).

## 4. Discussion

Gel-PCL fibrillar scaffolds with 30 and 45 wt.% Gel were successfully electrospun using an environmentally friendly, single-step solution procedure, where AcAc was used as a “green” sole solvent to straightforwardly produce Gel-PCL solutions with Gel concentration ≥ 30 wt.% and suitable for electrospinning. The electrospun scaffolds presented fibrillar morphologies with average fiber diameters that significantly decreased upon Gel addition to the scaffolds, in comparison to o-PCL; that is, micron average fiber diameters for o-PCL and submicron average fiber diameter for 30Gel/PCL and

45Gel/PCL scaffolds were observed. Similar effects, about the sub-micron average fiber diameter obtained and its decrement with Gel concentration were also observed before for Gel-PCL electrospun scaffolds from solutions of different solvents than AcAc. Studies showing PCL-Gel scaffolds with ≈ 50 wt.% Gel evidenced significantly inhomogeneous fiber morphologies with highly dispersed fiber diameter distribution (9,10,22). According to Feng et al. (28), the decrement in fiber diameter with Gel concentration might be ascribed to the increment of charge density in Gel-PCL AcAc-doped TFE solutions due to Gel addition since PCL is a non-ionic synthetic polymer and it is not expected to produce significant additional charges upon dissolution in AcAc. In the present work a considerable increment in the conductivity of the Gel-PCL-AcAc blend electrospinning solutions, in comparison to only-PCL-AcAc solutions, was observed, this increment was positively correlated with the increment in Gel concentration for the solutions; Table 1. At low pH (AcAc, pH ≈ 2.4), amino groups in amphoteric Gel molecules can be easily protonated producing positive charges (39) that increase the overall charge density, and therefore, the conductivity of the Gel-PCL-AcAc blend solutions. It is well known that in the electrospinning process an increase in conductivity causes greater elongation forces resulting in fibers of smaller diameter (56). Then, as Gel concentration increased, conductivity (charge density) further increased, which favored the formation of fibers with smaller diameters for 45Gel/PCL and 30Gel/PCL in comparison to o-PCL. As Gel concentration in the electrospinning solutions increased, viscosity of solutions decreased (Table 1), which could have also further contributed to facilitate the electrospinning process and the formation of thinner fibers for the Gel-PCL blend scaffolds.

Non-homogeneous, phase-separated, natural-synthetic polymer solutions normally result in electrospun scaffolds with inhomogeneous fiber morphology (54); the more critical the phase separation, the larger the scaffold's fiber inhomogeneity. 30Gel/PCL and 45Gel/PCL scaffolds showed

smooth, uniform, narrow fibers with similar characteristics to those of fibrillar scaffolds obtained from TFE-based, chloroform-methanol or hexafluoropropanol multi step electrospinning solutions (9,10,22,28,57). This result is in line with the observation that Gel-PCL-AcAc solutions in the present study did not present significant phase-separation.

PCL is a polyester with characteristic IR bands at 2900-2800, 1730-1750 and 1150 $cm^{-1}$ that correspond to the C-H, C=O-O and C-O stretching, respectively (9,10,32,58). Nevertheless, the FTIR-spectra of as-electrospun o-PCL scaffolds showed an additional band at 3480 $cm^{-1}$ that can be assigned to O-H stretching. In this respect, the strong acidity of the AcAc might had induced a slight PCL degradation during the dissolution process, increasing the number of PCL chains terminal O-H groups (59). However, the more likely cause for the observation of OH groups can be an inadequate evaporation of the AcAc during the electrospinning process (even after two weeks of scaffolds drying). Washed scaffolds, as used for the *in vitro* studies, were assessed before and after UV-sterilization, and in this case the IR spectra of o-PCL showed no FTIR bands that can be associated to OH groups, confirming that observation of the OH-stretching band in the spectra of the as-electrospun o-PCL was due to the presence of AcAc traces in the scaffold. Above 3000 $cm^{-1}$, pristine Gel showed a broad band centered at ≈ 3438 $cm^{-1}$ corresponding to N-H stretching (32); however, the FT-IR spectra of the Gel-PCL scaffolds showed a broad band centered at 3296 $cm^{-1}$. Shifting of this band towards lower wavenumbers (3296 $cm^{-1}$) respect to pristine Gel (3438 $cm^{-1}$) might be accounted for by protonation of the amino groups of Gel and/or indicate hydrogen bonds interactions between PCL and Gel as previously reported (32,34). PCL chains susceptibility to form hydrogen bonds with Gel N-H groups could have contributed to facilitate Gel-PCL miscibility.

Among tissue engineering scaffold properties, wettability is relevant because hydrophilicity is usually expected to be beneficial for cell adhesion and proliferation, and thus, hydrophilic scaffolds could be expected to be feasible for enhancing wound healing upon a potential patient application as scaffolds for skin tissue engineering (60,61). In agreement with previous reports by other authors (10,22,42), the present results showed that integration of Gel to the scaffolds induced the formation of hydrophilic surfaces, where WCA, as measured on fully hydrated samples, significantly decreased with the increment of the scaffolds' Gel concentration. As expected, due to the hydrophobic nature of PLC, o-PCL scaffolds were hydrophobic showing a high WCA (≈ 140° on hydrated samples) that rapidly stabilized at 126.6°. 30Gel/PCL and 45Gel/PCL scaffolds showed a hydrophilic nature (WCA < 90°), exhibiting WCA values for the 30Gel/PCL and 45Gel/PCL hydrated samples (65.1° and 25.3°, respectively for 30Gel/PCL and 45Gel/PCL) significantly smaller than those of hydrated o-PCL scaffolds. The water uptake capacity of the Gel/PCL blend scaffolds was also significantly enhanced in comparison to o-PCL. PCL/Gel blend scaffolds water uptake significantly increased as Gel concentration in the scaffolds increased (Supplementary Figure S1), from the small water uptake capacity of o-PCL (10% swelling) to the 200% and 400% swelling (Supplementary Figure S1) observed for 30Gel/PCL and 45Gel/PCL, respectively.

Dry Gel/PCL scaffolds presented a rapid water absorption, where after 5 s of water droplet deposition on the surface of these samples, the water droplet was almost completely absorbed by the scaffolds. On the other hand, o-PCL scaffolds hydrophobic surface prevented water-surface appropriate interactions resulting in very small water absorption, where after 5 s of water contact with dry o-PCL samples, the round shape of the water droplet deposited still remained quite stable (WCA = 134). Improvement of water wettability of 30Gel/PCL and 45Gel/PCL in comparison to o-PCL can be

mainly ascribed to the contribution of the polar nature of the Gel component in the Gel-PCL blend scaffolds. Gel possesses amide bonds and hydrophilic carboxylic and amine functional groups that allow interaction and formation of hydrogen bonds with water molecules, resulting in the hydrophilic nature observed for the Gel/PCL blend scaffolds and their significantly increase in water uptake capacity, in comparison to o-PCL.

Thermal stability of the obtained scaffolds was evaluated through TGA measurements, which provided also qualitative indication on the scaffolds' composition. The o-PCL scaffolds showed a single-step thermal degradation profile at $T_{max}$ of 394 °C, whereas pristine Gel showed multiple peaks of weight loss due to the loss of absorbed water and the Gel thermal degradation due to protein chain breakage and peptide bonds rupture (62,63). Moreover, Gel was not fully degraded after 700 °C, since a weight residual of about 20% was observed. The observation of the contribution of both components, Gel and PCL, in the thermal degradation of the blend scaffolds corroborated that both components PCL and Gel were present blended in the scaffolds. The calorimetric behavior of the 30Gel/PCL and 45Gel/PCL scaffolds showed a unique melting temperature at ≈ 55 °C which was attributed to PCL. The absence of the characteristic peak of Gel (≈ 93 °C) in the thermograms of the Gel-PCL scaffolds suggested that Gel was well dispersed at the molecular level within PCL, evidencing a good miscibility between both materials (64). From the calculated percentage of crystallinity from the $\Delta H_m$ and from qualitative analysis of the XRD patterns, it can be deduced that the overall crystallinity of the scaffolds decreased with the increment of Gel concentration in the scaffolds. As mentioned above, the use of AcAc as solvent for the electrospinning solutions can improve Gel protonation, as suggested by the increment in the conductivity of the Gel-PCL solutions in comparison to pure PCL solutions. Improved Gel protonation is expected to enhance Gel chains stretching due to electrostatic repulsions,

which can consequently favor Gel chains penetration into the PCL chains enhancing their miscibility. However, this phenomenon did not restrict PCL chain mobility and its ability for crystallization remained unaltered, and the presence of Gel in the blends simply "dilute" the crystalline phase in the scaffolds. The absence of interference of Gel into the ability of PCL to crystallize (to the same extent as in the pure PCL state) in the blend scaffolds was demonstrated by the calculated values of the melting enthalpy per gram of PCL present in each blend scaffold [ΔHm(PCL)] which remained almost the same for all Gel:PCL ratio. In line with this result, the smaller intensity of XRD peaks at 2Θ = 21.11° and 23.99° (attributed to PCL) for Gel-PCL scaffolds in comparison to o-PCL, can be ascribed to the higher content of amorphous component in the scaffolds as Gel concentration increased.

A. Papa et al. (23) fabricated electrospun fibrillar Gel-PCL mats with 50 wt.% Gel by means of a two-step solution process using HFP as solvent. Mats showed two endothermic peak temperatures corresponding to PCL and Gel (Gel $T_m$ was a low-intensity broad peak, but it was still observed in the DSC scans) indicating not complete miscibility of Gel-PCL. Not complete miscibility of HFP Gel-PCL solutions was also corroborated by Kolbuk et al. (27). The non-linear Tm dependence on the PCL:Gel ratio observed by Kolbuk et al. suggested that PCL-Gel-HFP solution systems were compatible (sufficiently strong PCL-Gel interaction) but not completely miscible (27). Enhancement of Gel-PCL blending was demonstrated in previous studies by Zhou, Q. et al. and Feng, B. et al. where alkali- or acid-doped solutions were used (28,54), showing the presence of a single $T_m$ (close to PCL $T_m$ = 59 °C) or no presence of the $T_m$ peak associated to Gel (≈ 93.9 °C). According to Mohamed et al. (64) it is possible to state that the present PCL-Gel electrospun scaffolds obtained from AcAc solutions represent miscible blends, displaying a single $T_m$ that was composition dependent (increasing with Gel concentration) in the evaluated temperature and composition ranges.

In the present work, the use of AcAc as the sole solvent for the electrospinning solutions did not seem to affect the mechanical strength of the present o-PCL scaffolds, in comparison to PCL scaffolds electrospun from solutions of different organic solvents, other than sole AcAc. o-PCL scaffolds in the present work showed E = 4.07 MPa, $\sigma_{max}$ = 1.21 MPa and ε = 93.27% in their hydrated state and E = 6.09 MPa, $\sigma_{max}$ = 2.27 MPa and ε = 238.2% in its dry state which is in agreement with mechanical properties reported for PCL scaffolds electrospun from TFE or chloroform solutions, that displayed E = 1.43-4.98 MPa, $\sigma_{max}$ = 1.2-2.7 MPa and ε = 48-126%, depending on whether the mechanical properties were assessed in dry or hydrated samples [15,21,24,27].

When Gel is blended with PCL, the mechanical properties of resulting Gel-PCL electrospun scaffolds can vary within a wide range depending on the chemical characteristics of the scaffolds such as Gel:PCL composition ratio and degree of Gel-PCL miscibility, and some morphological features such as fibers diameter, orientation or configuration (coaxial, single composition or co-electrospinning) (10,11,28,37,54). Nevertheless, in the case of Gel/PCL scaffolds, samples hydration state (dry or hydrated) is a key factor greatly influencing the mechanical properties, with different hydration conditions resulting in significantly different tensile properties for the same scaffold. Previous works have reported elastic modulus for dry Gel/PCL scaffolds in the range of 2.7 to 154.7 MPa, mainly depending on Gel:PCL composition ratio and miscibility. In contrast, for hydrated Gel/PCL scaffolds elastic modulus have been reported in the range of 0.5 to 15 MPa (10,11,37,45,54). In the present work, elastic modulus of Gel/PCL scaffolds dropped from 12.66 and 49.56 MPa, respectively for 30Gel/PCL and 45Gel/PCL in the dry state to 6.01 and 7.23 MPa, respectively for 30Gel/PCL and 45Gel/PCL in the hydrated state. According to Vatankhah et al. model, elastic modulus of Gel/PCL scaffolds can be dropped by 80% under hydrated conditions in comparison to the same samples

assessed in dry conditions. The relative impact of Gel:PCL composition ratio, fibers diameter and fibers orientation in the mechanical properties of Gel/PCL scaffolds also change depending on the hydrated or dry state of the samples. In dry conditions, the most relevant factor is composition (45.4% relative impact) followed by fibers orientation and fiber diameter (33.9% and 20.7% relative impact, respectively), while in hydrated conditions, the relative impact of composition increases to 50.4% followed by fibers diameter and fiber orientation (34.7% and 14.9% relative impact, respectively) (37). The different mechanical properties of Gel/PCL scaffolds in dry and hydrated state can be mainly ascribed to the different mechanical nature of PCL and Gel in dry and hydrated conditions. While PCL is a mainly elastic polymer in either dry or hydrated state, Gel is a stiff and brittle biopolymer in the dry state but presents a plastic behavior in hydrated conditions (37) with mechanical properties reported as E = 0.4-0.8 MPa, $\sigma_{max}$ = 0.2-0.5 MPa and ε = 150-90% for crosslinked Gel electrospun scaffolds in the hydrated state and E = 45-105 MPa, σ = 1.1-2.5 MPa and ε = 5-64% for Gel scaffolds in the dry state (24,36,39). The significant differences observed in the elastic modulus of Gel scaffolds in hydrated and dry state have been mainly ascribed to the high Gel hydration capacity (37,54).

The remarkably different properties of Gel/PCL scaffolds in dry and hydrated conditions emphasize the importance of assessing the mechanical properties of Gel/PCL scaffolds in their hydrated state, which better resembles the *in vitro* and *in vivo* conditions of scaffolds intended for tissue engineering applications. In the present work, blending of Gel and PCL resulted in electrospun scaffolds that presented in hydrated conditions, significantly higher elongation at break but comparable elastic modulus and maximum tensile strength than that of the o-PCL scaffolds. This can be explained in terms of the Gel hydrophilicity and high capability of water absorption, the intermolecular interactions between Gel and PCL (FT-IR results) and the decrement of the overall (as

blend bulk material) Gel-PCL scaffolds crystallinity degree (DSC results) due to Gel incorporation (amorphous component). Finally, it is important to emphasize that tensile moduli in hydrated conditions of present Gel/PCL scaffolds was within the range of elastic moduli reported for the skin (E = 0.06 – 70 MPa, depending on the body area and measurement conditions (11,37,65)). Also, according to Duan et al. membranes with E > 1.3 MPa and $\sigma_{max}$ > 1.5 MPa in hydrated conditions, as it is the case of the present Gel/PCL scaffolds, have potential to meet the mechanical requirements for temporary wound covers intended for skin regeneration (36), which are not normally subjected to high tensile strength when immobilized at wound sites (66). Thus, the present Gel/PCL scaffolds exhibited feasible mechanical properties as potential tissue engineering scaffolds for wound healing.

As previously mentioned, acidic pH of AcAc facilitated Gel protonation, as a consequence, strong physical interactions (hydrogen bonding) between Gel and PCL occurred, facilitating Gel interaction with PCL chains and enhancing the blending of these two polymers. Blending increase polymer chain entanglement and resulted in homogeneous and thermally stable Gel-PCL scaffolds with thinner fibers. It should be noted that even though secondary intermolecular bonds such as hydrogen bonds are much weaker than primary covalent bonds, significant intermolecular forces can result from the formation of many hydrogen inter-chain bonds which are capable of resisting polymer chains displacement (65). Hence, Gel-PCL enhanced interactions restricted PCL chains displacement and consequently the elastic modulus of Gel-PCL scaffolds increased in comparison to that of o-PCL. The elastic moduli and elongation at break of the present Gel-PCL scaffolds are within similar values to those previously reported for Gel-PCL scaffolds with 50 wt.% Gel electrospun from AcAc-doped TFE solutions (28,39). However, the blending of Gel and PCL did not considerably affect the maximum tensile strength of o-PCL scaffold ($\sigma_{max}$ ≈ 0.96 - 1.21 MPa) suggesting a homogeneous gelatin inclusion

in the PCL molecular chains. According to Duan et al. membranes with E = 1.5 MPa and σ = 1.3 MPa in wet state, have potential to meet the mechanical requirements for temporary wound covers intended for skin regeneration (36). Thus, the elastic modulus of the present Gel-PCL scaffolds meet the mechanical parameter of the skin: E = 0.06 – 70 MPa, (depending on the body area and/or measurement conditions) (11,37,65). Therefore, present Gel-PCL scaffolds represent a potential option as skin tissue engineering scaffolds that could also simultaneously function as temporary wound covers. Gel incorporation improved the elongation at break of the Gel-PCL scaffolds in comparison to o-PCL resulting in more flexible materials. This could be because the polar groups of Gel formed extra hydrogen bonding with water molecules, thereby, increasing their plasticity properties.

Since Gel is a water-soluble protein, crosslinking of Gel-based scaffolds is commonly used to prevent rapid dissolution of the scaffolds in biological media. Nevertheless, some techniques for Gel crosslinking have been associated to potential cytotoxic effects due to the presence of crosslinking agent residues when appropriate purification protocols after crosslinking are not implemented (67,68). In the present work, no crosslinking was implemented to avoid potential toxic effects, and to evaluate whether straightforward Gel blending with PCL by electrospinning from sole AcAc Gel-PCL solutions could increase the stability of Gel towards water dissolution in an appropriate range for scaffolds intended for skin tissue engineering capable of promoting cell adhesion and proliferation of fibroblast. The rate of Gel dissolution into aqueous media at 37°C, as determined by Biuret assay, of the present Gel-PCL scaffolds was lower than dissolution rates reported in the literature for non-crosslinked only-Gel electrospun scaffolds, which were totally dissolved after 1 h (69). A. Papa et al. used glyceraldehyde (GC) and 1,4-butanediol diglycidyl ether (BDDGE) for Gel crosslinking into PCL-Gel electrospun fibers, reporting that scaffolds crosslinked with BDDGE (≈ 20% of crosslinking degree)

showed a complete release of total Gel after just few hours of incubation in deionized water at 37°C, while scaffolds crosslinked with GC (≈ 30% of degree of crosslinking) showed a release of ≈ 44% of Gel content after ≈ 75 h under the same conditions (23). Kishan. et al. reported that Gel electrospun fibers crosslinked *in situ* with hexamethylene diisocyanate (≈ 32% of degree of crosslinking) lost ≈ 56% and 75% of its mass, respectively, after ≈ 24 and 72 h of immersion in an enzymatic solution (collagenase-PBS) at 37°C (24). In comparison to those previous studies, it can be suggested that present Gel-PCL scaffolds displayed a moderated Gel dissolution rate, showing slower Gel dissolution rates than those showed by only-Gel electrospun fibers with no crosslinking or Gel-PCL electrospun fibers crosslinked with BDDGE (20% of crosslinking degree) (23,69), but showing faster Gel dissolution rates than Gel electrospun fibers crosslinked *in situ* with hexamethylene diisocyanate (32% of degree of crosslinking) (24). Moderate Gel stability in aqueous solutions at 37°C of present scaffolds might be addressed to improved miscibility and intermolecular forces between PCL and Gel due to the use of AcAc as the sole solvent for the electrospinning solutions. Other factors such as a slow diffusion of Gel from the inner parts of the scaffolds to the surface/exposed areas of the scaffolds could also be influencing the slower Gel dissolution rate in aqueous media observed from the present blend Gel-PCL scaffolds in comparison to crosslinked only-Gel scaffolds or some crosslinked PCL-Gel scaffolds.

Gel-PCL scaffolds underwent a faster weight loss ($W_{loss}$) in comparison to o-PCL scaffolds during the first 3 days of immersion. A small weight loss for o-PCL scaffolds (about 4%) occurred during the first 3 days of incubation and no further significant $W_{loss}$ increments occurred for the time investigated in the present study (17 days). $W_{loss}$ observed for Gel-PCL scaffolds mainly corresponded to the amount of Gel released from the scaffolds as estimated from Biuret assay, indicating that $W_{loss}$ of 30Gel/PCL and 45Gel/PCL scaffolds during immersion can be mainly ascribed to Gel dissolution. The polar nature

of Gel molecules decreased 30Gel/PCL and 45Gel/PCL scaffolds hydrophobicity in comparison to o-PCL scaffolds, which might had also contributed to facilitate the scaffolds water uptake, and thus, to increase the PCL degradation rate, which occurs mainly through hydrolysis (16).

MTT-Formazan assays exhibited a larger number of cells on 30Gel/PCL and 45Gel/PCL scaffolds in comparison to o-PCL scaffolds. Cell viability improvement did not show any significant differences between scaffolds after 1 day of cell culture. Nevertheless, number of cells on the scaffolds was positively correlated to the amount of Gelatin in the 30Gel/PCL and 45Gel/PCL scaffolds after 3 days of cell culture and the number of cells was significantly higher on 45Gel/PCL than on o-PCL scaffolds at 3 and 7 days of culture. Considering that at 1 day of culture the number of cells on 30Gel/PCL and 45Gel/PCL were not significantly different from that on o-PCL scaffolds; then, MTT-Formazan assay results at 3 and 7 days of cell culture suggested that Gel induces a significant increment in fibroblasts proliferation on the scaffolds. Cell viability improvement with Gel concentration, in comparison to o-PCL scaffolds, can be ascribed to both the Gel in the scaffolds and the Gel released into the local microenvironment upon cell culture, since Gel has proved its ability to promote integrin binding sites, and hydrophilic amine and carboxyl functional groups for cell differentiation and adhesion (70). In agreement with these Gel properties, different studies have reported that Gel-PCL fibers promote cell adhesion and proliferation in comparison to pristine PCL fibers (10,22,40). In the present study, fluorescent micrographs from LIVE/DEAD assays on cell-cultured o-PCL scaffolds showed viable cells that mainly remained in the area where they were originally drop-seeded. This agglomeration-like behavior can be explained by the hydrophobic nature of the o-PCL scaffolds. In contrast, on the hydrophilic 30Gel/PCL and 45Gel/PCL scaffolds cells homogeneously extended all over the surface of the scaffolds with culture days. In agreement with viability assays, SEM analysis showed a well-adhered

and dense layer of fibroblast on PCL-Gel blend scaffolds at all culture time points studied. At 7 days of culture, a uniform dense layer of cells and secreted ECM components was observed on 30Gel/PCL scaffolds almost covering the entire surface of the scaffold. Fibroblasts are the most abundant cells in the dermis, and in a favorable environment, these cells synthesize the dermis ECM that is mainly composed of elastin and collagen Type I fibers (71). Immunocytochemistry assays performed in the present study showed that human fibroblast cultured on o-PCL, 30Gel/PCL and 45Gel/PCL scaffolds positively synthetized tropoelastin and collagen Type I at a similar level than fibroblasts cultured in monolayer on tissue culture plates. These qualitative results can be seen as an indication that fibrillar morphology and chemical composition of the present scaffolds was favorable for culturing human fibroblasts.

## 5. Conclusions

Homogeneous Gel-PCL blend fibrillar scaffolds were successfully fabricated by electrospinning using an AcAc sole solvent straightforward approach that, to the best of our knowledge, was applied here for the first time to electrospun Gel-PCL solutions with Gel concentration $\geq$ 30 wt.%. Physical-chemical characterization of the scaffolds showed that Gel and PCL interacted mainly by hydrogen bonds resulting in miscible blend Gel-PCL scaffolds. Most likely, the miscibility of the synthetic-natural polymer blends was a result of the strong acidity of AcAc that improved the protonation of the of Gel molecules in the electrospinning solutions. Miscibility of Gel-PCL in the blend scaffolds decreased the dissolution rate of Gel in aqueous solution (PBS, pH 7.4) at 37°C, improving the stability of the scaffolds. Furthermore, scaffolds biological response assessment with fibroblasts confirmed their

biocompatibility and the feasibility of the Gel-PCL blend scaffolds to promote fibroblasts adhesion and proliferation. The developed Gel-PCL fibrillar membranes showed potential application in the tissue engineering field as scaffolds for wound healing. Among the scaffolds studied, 30Gel/PCL was demonstrated to be the best candidate for tissue engineering applications, satisfying better the expected mechanical, stability and biocompatibility requirements.

## Supplementary Figures

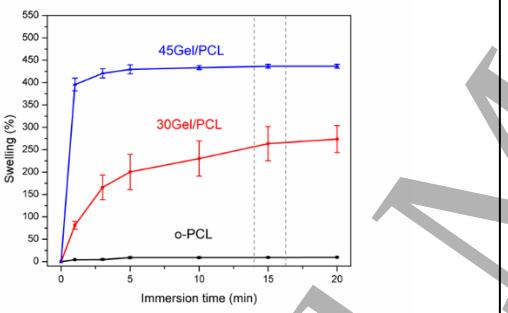


**Supplementary Figure S1.** Swelling in percentage of o-PCL, 30Gel/PCL and 45Gel/PCL scaffolds *vs.* immersion time in double distilled water. Swelling was calculated as $[(W_t - W_{t=0}) / W_{t=0}]*100$; where $W_t$ corresponds to hydrated samples weight at each immersion time and $W_{t=0}$ corresponds to initial dry samples weight before immersion in distilled water.

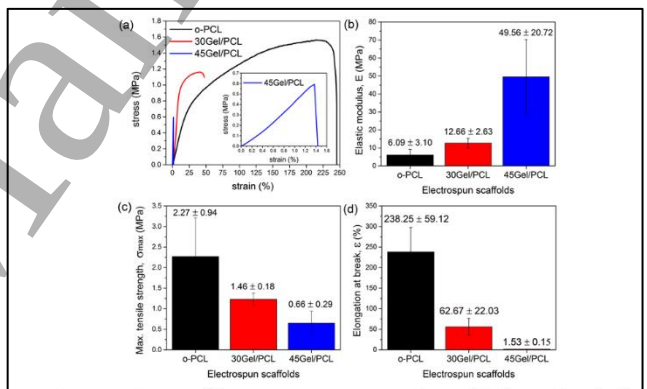


**Supplementary Figure S2.** (a) Typical stress-strain curves of o-PCL (black), 30Gel/PCL (red) and 45Gel/PCL (blue and inset) scaffolds in their dry state and their corresponding mechanical parameters calculated from the strain-stress curves: (b) elastic modulus, E; (c) maximum tensile strength, $\sigma_{max}$; and (d) elongation at break, Ɛ.

## Acknowledgments

The authors acknowledge the Scanning Electron Microscopy technical support of Omar Novelo-Peralta from the Instituto de Investigaciones en Materiales at UNAM, Mexico and Samuel Tehuacanero-Cuapa, Roberto Hernández-Reyes and Diego Quiterio-Varga from the Instituto de Física at UNAM, México. The authors also acknowledge the Universal Testing Machine technical support of Eliezer Hernández

Mecinas from the Instituto de Investigaciones en Materiales at UNAM, Mexico. The authors acknowledge general laboratory technical support from Xochitl Guerrero from the Instituto Nacional de Rehabilitación-LGII, México. The support and advice of B.Sc. Julieta García-López (inmmunocytochemistry assays) and M.Sc. Valentín Martínez-López (*in vitro* biocompatibility assays) from the Instituto Nacional de Rehabilitación-LGII, Mexico is also acknowledged. The scientific advice of Dr. Sandra E. Rodil from the Instituto de Investigaciones en Materiales at UNAM, Mexico is gratefully acknowledged. G. Prado-Prone acknowledges financial support from CONACyT post-graduate and mixed scholarship number 443935. G. Prado-Prone also acknowledge the postdoctoral fellowship (POSDOC program) provided by DGAP-UANM. This project was partly funded by Instituto Nacional de Rehabilitación-LGII, PAEP-IIM-UNAM 2017, CONACyT Project 179607, SECITI/053/2016, Bilateral México-Italia 234789. The Italian Ministry of University and Research (MIUR) is also acknowledged.

## References

1. Zou L, Zhang Y, Liu X, Chen J, Zhang Q. Biomimetic mineralization on natural and synthetic polymers to prepare hybrid scaffolds for bone tissue engineering. Colloids Surfaces B Biointerfaces. 2019;178:222–9.
2. Aldana AA, Abraham GA. Current advances in electrospun gelatin-based scaffolds for tissue engineering applications. Int J Pharm. 2017;523(2):441–53.
3. Tabasum S, Noreen A, Maqsood MF, Umar H, Akram N, Nazli Z i. H, et al. A review on versatile applications of blends and composites of pullulan with natural and synthetic polymers. Int J Biol Macromol. 2018;120:603–32.
4. Salehi M, Farzamfar S, Bozorgzadeh S, Bastami F. Fabrication of Poly(L-Lactic Acid)/Chitosan Scaffolds by Solid-Liquid Phase Separation Method for Nerve Tissue Engineering: An In Vitro Study on Human Neuroblasts. J Craniofac Surg. 2019;30(3):784–9.
5. Sharma V, Patel N, Kohli N, Ravindran N, Hook L, Mason C, et al. Viscoelastic, physical, and bio-

degradable properties of dermal scaffolds and related cell behaviour. Biomed Mater. 2016;11(5).

6. Catalano E, Cochis A, Varoni E, Rimondini L, Azzimonti B. Tissue-engineered skin substitutes: an overview. J Artif Organs. 2013;16(4):397–403.

7. Zhong SP, Zhang YZ, Lim CT. Tissue scaffolds for skin wound healing and dermal reconstruction. Wiley Interdiscip Rev Nanomedicine Nanobiotechnology. 2010;2(5):510–25.

8. Goodarzi P, Falahzadeh K, Nematizadeh M, Farazandeh P, Payab M, Larijani B, et al. Tissue Engineered Skin Substitutes BT - Cell Biology and Translational Medicine, Volume 3: Stem Cells, Bio-materials and Tissue Engineering. In: Turksen K, editor. Cham: Springer International Publishing; 2018. p. 143–88.

9. Ferreira P, Santos P, Alves P, Carvalho MP, de Sá KD, Miguel SP, et al. Photocrosslinkable electrospun fiber meshes for tissue engineering applications. Eur Polym J. 2017;97(October):210–9.

10. Jiang YC, Jiang L, Huang A, Wang XF, Li Q, Turng LS. Electrospun polycaprolactone/gelatin composites with enhanced cell?matrix interactions as blood vessel endothelial layer scaffolds. Mater Sci Eng C. 2017;71:901–8.

11. Fu Y, Guan J, Guo S, Guo F, Niu X, Liu Q, et al. Human urine-derived stem cells in combination with polycaprolactone/gelatin nanofibrous membranes enhance wound healing by promoting angiogenesis. J Transl Med. 2014;12(1):274.

12. Dubský M, Kubinová Š, Širc J, Voska L, Zajíček R, Zajícová A, et al. Nanofibers prepared by needleless electrospinning technology as scaffolds for wound healing. J Mater Sci Mater Med. 2012;23(4):931–41.

13. Qasim SB, Zafar MS, Najeeb S, Khurshid Z, Shah AH, Husain S, et al. Electrospinning of chitosan-based solutions for tissue engineering and regenerative medicine. Int J Mol Sci. 2018;19(2).

14. Soares RMD, Siqueira NM, Prabhakaram MP, Ramakrishna S. Electrospinning and electrospray of bio-based and natural polymers for biomaterials development. Mater Sci Eng C [Internet]. 2018;(November 2017):0–1. Available from: https://doi.org/10.1016/j.msec.2018.08.004

15. Araujo J V., Carvalho PP, Best SM. Electrospinning of bioinspired polymer scaffolds. In: Advances in Experimental Medicine and Biology. 2015.

16. Woodruff MA, Hutmacher DW. The return of a forgotten polymer—Polycaprolactone in the 21st century. Prog Polym Sci [Internet]. 2010 Oct 1 [cited 2018 Mar 2];35(10):1217–56. Available from: https://www.sciencedirect.com/science/article/pii/S0079670010000419?via%3Dihub

17. Kim CH, Khil MS, Kim HY, Lee HU, Jahng KY. An improved hydrophilicity via electrospinning for enhanced cell attachment and proliferation. J Biomed Mater Res - Part B Appl Biomater. 2006;78(2):283–90.

18. Gomes SR, Rodrigues G, Martins GG, Roberto MA, Mafra M, Henriques CMR, et al. In vitro and in vivo evaluation of electrospun nanofibers of PCL, chitosan and gelatin: A comparative study. Mater Sci Eng C [Internet]. 2015;46:348–58. Available from:

http://dx.doi.org/10.1016/j.msec.2014.10.051

19. Van Doren SR. Matrix metalloproteinase interactions with collagen and elastin. Vols. 44–46, Matrix Biology. 2015. p. 224–31.

20. Van Vlierberghe S, Vanderleyden E, Boterberg V, Dubruel P. Gelatin functionalization of biomaterial surfaces: Strategies for immobilization and visualization. Polymers (Basel). 2011;3(1):114–30.

21. Başaran İ, Oral A. Grafting of poly(ε-caprolactone) on electrospun gelatin nanofiber through surface-initiated ring-opening polymerization. Int J Polym Mater Polym Biomater. 2018;(January):1–8.

22. Feng B, Duan H, Fu W, Cao Y, Zhang WJ, Zhang Y. Effect of inhomogeneity of the electrospun fibrous scaffolds of gelatin/polycaprolactone hybrid on cell proliferation. J Biomed Mater Res - Part A. 2015;103(2):431–8.

23. Papa A, Guarino V, Cirillo V, Oliviero O, Ambrosio L. Optimization of Bicomponent Electrospun Fibers for Therapeutic Use: Post-Treatments to Improve Chemical and Biological Stability. J Funct Biomater. 2017;8(4):47.

24. Kishan AP, Nezarati RM, Radzicki CM, Renfro AL, Robinson JL, Whitely ME, et al. In situ crosslinking of electrospun gelatin for improved fiber morphology retention and tunable degradation. J Mater Chem B. 2015;3(40):7930–8.

25. Xue J, Feng B, Zheng R, Lu Y, Zhou G, Liu W, et al. Engineering ear-shaped cartilage using electrospun fibrous membranes of gelatin/polycaprolactone. Biomaterials. 2013;34(11):2624–31.

26. Fee T, Surianarayanan S, Downs C, Zhou Y, Berry J. Nanofiber alignment regulates NIH3T3 cell orientation and cytoskeletal gene expression on electrospun PCL+gelatin nanofibers. PLoS One [Internet]. 2016;11(5):1–12. Available from: http://dx.doi.org/10.1371/journal.pone.0154806

27. Kolbuk D, Sajkiewicz P, Denis P, Choinska E. Investigations of polycaprolactone/gelatin blends in terms of their miscibility. Bull Polish Acad Sci Tech Sci. 2013;61(3):629–32.

28. Feng B, Tu H, Yuan H, Peng H, Zhang Y. Acetic-acid-mediated miscibility toward electrospinning homogeneous composite nanofibers of GT/PCL. Biomacromolecules. 2012;13(12):3917–25.

29. Bhat V, Shivakumar HR, Sheshappa RK, Sanjeev G. Preparation and study on miscibility, thermal behavior of biocompatible polymer blends of xanthan Gum-polyacrylamide. Int J Plast Technol. 2014;18(2):183–91.

30. Chang R, Lata R, Rohindra D. Miscibility study of poly(butylene succinate) and pine-gum blends. Key Eng Mater. 2017;735 KEM:148–52.

31. Cailloux J, Abt T, García-Masabet V, Santana O, Sánchez-Soto M, Carrasco F, et al. Effect of the viscosity ratio on the PLA/PA10.10 bioblends morphology and mechanical properties. Express Polym Lett. 2018;12(6):569–82.

32. Gautam S, Chou CF, Dinda AK, Potdar PD, Mishra NC. Fabrication and characterization of PCL/gelatin/chitosan ternary nanofibrous composite scaffold for tissue engineering applications. J Mater Sci. 2014;49(3):1076–89.

33. Lanza R, Langer R, Vacanti JP. Principles of Tissue Engineering: Fourth Edition. Principles of Tissue Engineering: Fourth Edition. 2013. 1–1887 p.

34. Powell HM, Boyce ST. Engineered human skin fabricated using electrospun collagen-PCL blends: morphogenesis and mechanical properties. Tissue Eng Part A. 2009;15(8):2177–87.

35. Zhang YZ, Su B, Venugopal J, Ramakrishna S, Lim CT. Biomimetic and bioactive nanofibrous scaffolds from electrospun composite nanofibers. Vol. 2, International Journal of Nanomedicine. 2007. p. 623–38.

36. Duan H, Feng B, Guo X, Wang J, Zhao L, Zhou G, et al. Engineering of epidermis skin grafts using electrospun nanofibrous gelatin/polycaprolactone membranes. Int J Nanomedicine. 2013;8:2077–84.

37. Vatankhah E, Semnani D, Prabhakaran MP, Tadayon M, Razavi S, Ramakrishna S. Artificial neural network for modeling the elastic modulus of electrospun polycaprolactone/gelatin scaffolds. Acta Biomater. 2014;10(2):709–21.

38. Chen Z, Cao L, Wang L, Zhu H, Jiang H. Effect of fiber structure on the properties of the electrospun hybrid membranes composed of poly(ε-caprolactone) and gelatin. J Appl Polym Sci. 2013;127(6):4225–32.

39. Zhang Y, Ouyang H, Chwee TL, Ramakrishna S, Huang ZM. Electrospinning of gelatin fibers and gelatin/PCL composite fibrous scaffolds. J Biomed Mater Res - Part B Appl Biomater. 2005;72(1):156–65.

40. He X, Feng B, Huang C, Wang H, Ge Y, Hu R, et al. Electrospun gelatin/polycaprolactone nanofibrous membranes combined with a coculture of bone marrow stromal cells and chondrocytes for cartilage engineering. Int J Nanomedicine. 2015;10:2089–99.

41. Prado-Prone G, Silva-Bermudez P, Almaguer-Flores A, García-Macedo JA, García VI, Rodil SE, et al. Enhanced antibacterial nanocomposite mats by coaxial electrospinning of polycaprolactone fibers loaded with Zn-based nanoparticles. Nanomedicine Nanotechnology, Biol Med [Internet]. 2018;14(5):1695–706. Available from: https://doi.org/10.1016/j.nano.2018.04.005

42. Ferreira JL, Gomes S, Henriques C, Borges JP, Silva JC. Electrospinning polycaprolactone dissolved in glacial acetic acid: Fiber production, nonwoven characterization, and In Vitro evaluation. J Appl Polym Sci. 2014;41068:1–9.

43. Byrne FP, Jin S, Paggiola G, Petchey THM, Clark JH, Farmer TJ, et al. Tools and techniques for solvent selection: green solvent selection guides. Sustain Chem Process [Internet]. 2016;4(1):7. Available from: http://sustainablechemicalprocesses.springeropen.com/articles/10.1186/s40508-016-0051-z

44. Prado-Prone G, Silva-Bermudez P, Almaguer-Flores A, García-Macedo JA, García VI, Rodil SE, et

al. Enhanced antibacterial nanocomposite mats by coaxial electrospinning of polycaprolactone fibers loaded with Zn-based nanoparticles. Nanomedicine Nanotechnology, Biol Med. 2018;14(5).

45. Feng B, Tu H, Yuan H, Peng H, Zhang Y. Acetic-Acid-Mediated Miscibility toward Electrospinning Homogeneous Composite Nanofibers of GT / PCL Acetic-Acid-Mediated Miscibility toward Electrospinning Homogeneous Composite Nano fi bers of GT / PCL. Biomacromolecules. 2012;13(November):3917–25.

46. Denis P, Dulnik J, Sajkiewicz P. Electrospinning and Structure of Bicomponent Polycaprolactone/Gelatin Nanofibers Obtained Using Alternative Solvent System. Int J Polym Mater Polym Biomater. 2015;64(7):354–64.

47. Gautam S, Dinda AK, Mishra NC. Fabrication and characterization of PCL/gelatin composite nanofibrous scaffold for tissue engineering applications by electrospinning method. Mater Sci Eng C [Internet]. 2013;33(3):1228–35. Available from: http://dx.doi.org/10.1016/j.msec.2012.12.015

48. Taghizadeh A, Favis BD. Carbon nanotubes in blends of polycaprolactone/thermoplastic starch. Carbohydr Polym. 2013;98(1):189–98.

49. Shieh Y-T, Yang H-S, Chen H-L, Lin T-L. Nonisothermal crystallization of compatible PCL/PVC blends under supercritical CO2. Polym J. 2005;37(12):932–8.

50. Govor E, Oceli V, Slouf M, Šitum A. Characterization of Biodegradable Polycaprolactone Containing Titanium Dioxide Micro and. 2014;8(7):577–81.

51. Janairo G, Sy ML, Yap L, Llanos-lazaro N. Determination of the sensitivity range of biuret test for undergraduate biochemistry experiments. e-Journal Sci Technol. 2011;5(6):77–83.

52. Velasquillo C, Silva-Bermudez P, Vázquez N, Martínez A, Espadín A, García-López J, et al. In vitro and in vivo assessment of lactic acid-modified chitosan scaffolds for potential treatment of full-thickness burns. J Biomed Mater Res - Part A. 2017;105(10):2875–91.

53. Benkaddour A, Jradi K, Robert S, Daneault C. Grafting of Polycaprolactone on Oxidized Nanocelluloses by Click Chemistry. Nanomaterials. 2013;3(1):141–57.

54. Zhou Q, Zhang H, Zhou Y, Yu Z, Yuan H, Feng B, et al. Alkali-Mediated Miscibility of Gelatin/Polycaprolactone for Electrospinning Homogeneous Composite Nanofibers for Tissue Scaffolding. Macromol Biosci. 2017;1700268:1700268.

55. Abdelrazek EM, Hezma AM, El-khodary A, Elzayat AM. Spectroscopic studies and thermal properties of PCL/PMMA biopolymer blend. Egypt J Basic Appl Sci. 2016;3(1):10–5.

56. Son WK, Youk JH, Lee TS, Park WH. The effects of solution properties and polyelectrolyte on electrospinning of ultrafine poly(ethylene oxide) fibers. Polymer (Guildf). 2004;45(9):2959–66.

57. Gautam S, Chou CF, Dinda AK, Potdar PD, Mishra NC. Surface modification of nanofibrous polycaprolactone/gelatin composite scaffold by collagen type i grafting for skin tissue engineering. Mater Sci Eng C [Internet]. 2014;34(1):402–9. Available from:

http://dx.doi.org/10.1016/j.msec.2013.09.043

58. Lim MM, Sultana N. Comparison on in vitro degradation of polycaprolactone and polycaprolactone/gelatin nanofibrous scaffold. Malaysian J Anal Sci [Internet]. 2017;21(3):627–32. Available from: http://www.ukm.my/mjas/v21_n3/pdf/LimMimMim_21_3_12.pdf

59. Hernández AR, Contreras OC, Acevedo JC, Moreno LGN. Poly(ε-caprolactone) degradation under acidic and alkaline conditions. Am J Polym Sci. 2013;3(4):70–5.

60. Mikos AG, Lyman MD, Freed LE, Langer R. Wetting of poly(l-lactic acid) and poly(dl-lactic-co-glycolic acid) foams for tissue culture. Biomaterials. 1994;15(1):55–8.

61. Sood A, Granick MS, Tomaselli NL. Wound Dressings and Comparative Effectiveness Data. Adv wound care. 2014;3(8):511–29.

62. Li J, Ma J, Jiang T, Khan F, Wang Y, Chen Y, et al. Combined membrane emulsification with biomimetic mineralization: Designing and constructing novel organic-inorganic hybrid microspheres for enzyme immobilization. Compos Sci Technol. 2017;141:56–64.

63. Frazier SD, Srubar W V. Evaporation-based method for preparing gelatin foams with aligned tubular pore structures. Mater Sci Eng C. 2016;62:467–73.

64. Mohamed A, Finkenstadt VL, Gordon SH, Biresaw G, Palmquist Debra E, Rayas-Duarte P. Thermal properties of PCL/gluten bioblends characterized by TGA, DSC, SEM, and infrared-PAS. J Appl Polym Sci. 2008;110(5):3256–66.

65. Callister W, Rethwisch D. Materials science and engineering: an introduction. Vol. 94, Materials Science and Engineering. 2007. 538 p.

66. Zhang Q, Lv S, Lu J, Jiang S, Lin L. Characterization of polycaprolactone/collagen fibrous scaffolds by electrospinning and their bioactivity. Int J Biol Macromol [Internet]. 2015;76:94–101. Available from: http://dx.doi.org/10.1016/j.ijbiomac.2015.01.063

67. Yao R, He J, Meng G, Jiang B, Wu F. Electrospun PCL/Gelatin composite fibrous scaffolds: Mechanical properties and cellular responses. J Biomater Sci Polym Ed. 2016;27(9):824–38.

68. Guarino V, Altobelli R, Cirillo V, Cummaro A, Ambrosio L. Additive electrospraying: A route to process electrospun scaffolds for controlled molecular release. Vol. 26, Polymers for Advanced Technologies. 2015. p. 1359–69.

69. Torricelli P, Gioffrè M, Fiorani A, Panzavolta S, Gualandi C, Fini M, et al. Co-electrospun gelatin-poly(L-lactic acid) scaffolds: Modulation of mechanical properties and chondrocyte response as a function of composition. Mater Sci Eng C. 2014;36(1):130–8.

70. Samson M, Porter N, Orekoya O, Hebert JR, Adams SA, Bennett CL, et al. HHS Public Access. 2017;155(1):3–12.

71. Tracy LE, Minasian RA, Caterson EJ. Extracellular Matrix and Dermal Fibroblast Function in the Healing Wound. Adv Wound Care. 2014;